Food Chemistry 516 (2026) 149408

Contents lists available at ScienceDirect

Food Chemistry

journal homepage: www.elsevier.com/locate/foodchem

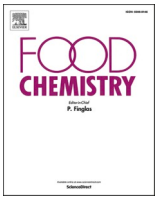

# pH-mediated hydrolysis alters phenolic profiles and biological functions of brown seaweeds

Xinyu Duan [a], Muthupandian Ashokkumar [b], Frank R. Dunshea [a,c], Hafiz A.R. Suleria [a,*]

[a] School of Agriculture, Food and Ecosystem Sciences, Faculty of Science, The University of Melbourne, Parkville, Australia
[b] School of Chemistry, Faculty of Science, The University of Melbourne, Parkville, Australia
[c] Faculty of Biological Sciences, The University of Leeds, Leeds, UK

ARTICLE INFO

*Keywords:*
Brown seaweeds
Matrix-bound phenolics
pH-assisted hydrolysis
Bioactivities
LC/Q-TOF MS

ABSTRACT

Phenolic compounds in brown seaweeds remain poorly characterized due to their complex associations with cell wall components. This study investigated the effects of pH-mediated hydrolysis (pH 1, 4, 10, and 13) on the release, composition, and bioactivities of bound phenolics from *Ascophyllum nodosum*, *Fucus vesiculosus*, and *Ecklonia radiata*, with their phenolic fractions as baselines. Phenolic content was quantified using complementary assays, and antioxidant, anti-diabetic, and anti-inflammatory activities were evaluated *in vitro*. Untargeted LC/Q-TOF MS profiling revealed pronounced pH- and species-dependent compositional differences. Alkaline hydrolysis (pH 10–13) released phenolic assemblages with superior radical scavenging and α-amylase inhibitory activity, whereas acidic conditions (pH 1–4) yielded phenolics with enhanced anti-inflammatory efficacy. This pattern demonstrated that extraction pH governs not merely phenolic yield but the functional identity of the liberated fraction. Correlation network analysis further confirmed the selective liberation of functionally coordinated phenolic assemblages upon hydrolysis.

## 1. Introduction

Brown seaweeds (Phaeophyceae) are a rich source of bioactive polyphenols that exhibit notable antioxidant, anti-inflammatory, and anti-diabetic activities (Duan et al., 2025). These polyphenolic compounds function as secondary metabolites in brown algae, contributing to ecological defense and environmental adaptation (Divekar et al., 2022). Owing to these multifunctional properties, brown seaweed polyphenols have attracted increasing attention for applications in nutraceuticals, functional foods, and pharmaceuticals (Cotas et al., 2020), driving the need for efficient extraction strategies that maximize recovery while preserving their bioactivity.

Phenolic compounds in brown seaweeds occur in both free (or soluble) and bound forms. Soluble phenolics include unconjugated compounds as well as solvent-extractable conjugated forms (e.g., esterified or etherified phenolics), whereas bound phenolics are covalently associated with structural polysaccharides (e.g., alginate, fucoidan) and proteins through ester, ether, or glycosidic bonds (Gunathilake et al., 2022; Krygier et al., 1982). Recent studies have shown that the bound-to-free phenolic ratio in brown seaweeds can range from 0.21 to 5.52, depending on species, with certain *Sargassum* species exhibiting ratios greater than 1 (Peng et al., 2024), indicating that bound phenolics may even predominate. Thus, basic solvent extraction may fail to recover a substantial proportion of phenolics, leading to underestimation of total phenolic content and associated bioactivities. Therefore, the importance of targeting bound phenolic fractions to achieve comprehensive functional evaluation is highlighted.

Hydrolysis-based approaches are commonly employed to release bound phenolics (Brglez Mojzer et al., 2016). Alkaline hydrolysis (1–4 M NaOH) is widely used due to its effectiveness in cleaving ester linkages (Gonzales et al., 2014; Irakli et al., 2018); however, high-concentration alkaline solutions may promote oxidation and structural degradation of phenolic compounds (Pasquet et al., 2024). Acidic hydrolysis can cleave glycosidic bonds but is less frequently applied and may also induce compound transformation under extreme conditions (Domínguez-Rodríguez et al., 2017). Most existing studies have compared only highly acidic and highly alkaline environments, leaving the effects of intermediate pH conditions largely unexplored. This gap is particularly consequential for brown seaweeds, whose cell walls harbor a unique combination of alginates, fucoidans, and phlorotannin-polysaccharide complexes with pH-sensitive binding chemistries distinct from those of terrestrial plants, which makes direct extrapolation of established

* Corresponding author.
*E-mail address:* hafiz.suleria@unimelb.edu.au (H.A.R. Suleria).

https://doi.org/10.1016/j.foodchem.2026.149408
Received 7 January 2026; Received in revised form 20 April 2026; Accepted 24 April 2026
Available online 26 April 2026

protocols both scientifically uncertain and practically unreliable.

Therefore, a systematic investigation of pH-dependent release patterns is required to clarify how hydrolysis intensity governs the liberation of bound phenolics and functional outcomes in brown seaweeds. To address this gap, we systematically examined how four incremental pH conditions (pH 1, 4, 10, and 13) shape the release, composition, and bioactivities of bound phenolics across three ecologically and commercially relevant brown seaweeds (*Ascophyllum nodosum, Fucus vesiculosus,* and *Ecklonia radiata*). Free phenolic fractions were characterized in parallel to serve as compositional and functional baselines against which the pH-dependent release of bound phenolics could be contextualized. Beyond quantifying phenolic yield and individual bioactivities, we further employed Mantel-based correlation network analysis to test whether pH-mediated hydrolysis selectively liberates functionally coordinated phenolic assemblages, rather than indiscriminately increasing phenolic load, which provided a mechanistic framework for pH-tailored extraction strategies and established a rational basis for the functional valorization of seaweed phenolics.

## 2. Materials and methods

### 2.1. Sample collection

Commercial dried seaweed powders of *Ascophyllum nodosum* (SKU: 209385–51) and *Fucus vesiculosus* (SKU: 209154–31) were purchased from Starwest Botanicals, Inc. (Sacramento, CA, USA), with a reported country of origin in Canada. *Ecklonia radiata* powder (Item code: 13235) was obtained from Pacific Harvest (Auckland, New Zealand), with a reported origin in New Zealand. These materials were commercially processed and supplied in sealed food-grade packaging. All samples were stored at -20 °C in a dark, dry environment until analysis and were used as received unless otherwise specified.

### 2.2. Extraction procedures

#### 2.2.1. Free phenolic fractions

The extraction of phenolic compounds from brown seaweeds was performed by sequential solvent extraction to obtain free and bound fractions. For free phenolics, dried seaweed powder was extracted with absolute methanol (1:10, *w/v*) using continuous shaking (200 rpm) for 16 h at room temperature, followed by centrifugation (4000 × *g*, 10 min, 4 °C). The supernatant was collected as the less-polar free phenolic fraction. The use of absolute methanol in this step was intended to selectively recover organic solvent-soluble free phenolics before any aqueous solvent was introduced. This extraction was repeated twice to maximize recovery. The residual pellets were washed and subsequently extracted with water under the same conditions to collect the water-soluble free phenolic fraction. Both fractions were combined to obtain the total free phenolic extract. The resulting combined extract approximated an 80% methanol system, which facilitated low-temperature precipitation (4 °C, overnight) and centrifugation (4000 × *g*, 10 min, 4 °C) for the removal of heteropolysaccharides as well as carbohydrates potentially soluble in organic solvents. However, it is acknowledged that low-temperature precipitation may result in partial co-precipitation of phenolic compounds as a minor limitation of the purification approach. The supernatant was collected for further analysis.

#### 2.2.2. Bound phenolic fractions

The residual pellets were washed twice with 100% methanol and hydrolyzed under acidic (pH 1 or 4) and alkaline (pH 10 or 13) conditions at 75 °C for 1 h, after which the released phenolics were extracted with methanol (added to the aqueous hydrolysate to achieve a hydro-alcoholic mixture suitable for phenolic recovery). The selected pH values spanned a gradient from strongly acidic to strongly alkaline conditions, enabling systematic evaluation of hydrolysis intensity. The temperature (75 °C) and duration (1 h) were adjusted based on previous studies reporting efficient cleavage of phenolic-matrix linkages while minimizing oxidative degradation (Antony & Farid, 2022; Irakli et al., 2018). These bound fractions were similarly processed through the same low-temperature precipitation steps as the free fractions. The supernatants were collected, neutralized, and extracted with an equal volume of ethyl acetate, and the extraction was repeated four times. The combined ethyl acetate fractions were evaporated to dryness using a rotary evaporator at 45 °C. Both free and bound fractions were separately concentrated to dryness and stored as powders at -20 °C for subsequent analyses.

### 2.3. Content determination

Total phenolic content (TPC), total phlorotannin content (TPhC), and total flavonoid content (TFC) were measured via Folin-Ciocalteu's assay, 2,4-dimethoxybenzaldehyde (DMBA) assay, and aluminum chloride colorimetric method, with adaptation based on Lee et al. (2024). Data were expressed as gallic acid equivalents (GAE), phloroglucinol equivalents (PGE), and quercetin equivalents (QE) per gram (dry weight), respectively.

Total tannin content (TTC) was measured using modified polyvinyl polypyrrolidone (PVPP) method based on its ability to bind tannin-phenolics, as proposed by Xia et al. (2023). 120 μL of each sample/standard was mixed with 180 μL of distilled water, 150 μL of Folin-Ciocalteu's reagent (50%, *v/v*), and 675 μL of sodium carbonate (20%, *w/v*) in the Eppendorf tubes. The mixture was vortexed and incubated in the dark at room temperature for 40 min. After incubation, the samples were centrifuged, and 200 μL of the supernatant was transferred to the 96-well microplate. Absorbance was measured at 725 nm. A standard calibration curve was constructed using tannic acid solutions in water (0–250 μg/mL). A second analysis was conducted to quantify non-tannin polyphenols of the samples. For this, 50 mg of PVPP was added to a mixture containing 500 μL of distilled water and 375 μL of the samples. After vortexing, the mixture was incubated at 4 °C for 15 min, then centrifuged at 4000 × *g* for 10 min at 4 °C. The resulting supernatant was analyzed using the same method described above. TTC was calculated by subtracting the non-tannin phenolic content from the total phenolic content. Final TTC values were expressed as milligrams of tannic acid equivalent (TAE) per gram of dry weight.

### 2.4. Biological activities

#### 2.4.1. Antioxidant activity

The 2,2′-diphenyl-1-picrylhydrazyl (DPPH) assay, ferric reducing antioxidant power (FRAP) assay, and ferrous ion chelating activity (FICA) assay were used to validate and provide a more comprehensive assessment of antioxidant potential through different mechanisms: free radical scavenging, electron donation (reducing power), and metal ion chelation, accordingly.

Concentration-dependent tests were conducted on all three assays, with each sample at 0.5 mg/mL, 1 mg/mL, 2 mg/mL, and 3 mg/mL. The specific experimental steps of DPPH and FRAP assays followed the protocol of a previous study (Duan et al., 2024). Data were expressed as μg Trolox/mL at each tested extract concentration to explicitly capture concentration-dependent response patterns across fractions and species; potency indices, including $IC_{50}$ and RC1.0 (defined as the extract concentration required to reach an absorbance of 1.0 at 593 nm in the FRAP assay, calculated by linear interpolation between the two nearest concentrations), are additionally provided in **SI. Table. S1 and SI. Table S2** to enable inter-fraction and inter-species comparisons independent of the tested concentration range.

The FICA assay was performed by mixing 15 μL of each sample/standard with 85 μL of distilled water, 50 μL of 0.125 mM ferrous chloride, and 50 μL of 0.7 mM ferrozine solution. The mixtures were incubated in the dark at 25 °C for 10 min. A standard calibration curve was generated using ethylenediaminetetraacetic acid (EDTA) solutions

ranging from 0 to 50 μg/mL. Absorbance was measured at 562 nm, and chelating activity was expressed as the EDTA concentration.

### 2.4.2. Anti-diabetic activity

*2.4.2.1. α-Glucosidase inhibitory activity.* The α-glucosidase inhibitory activity of different seaweed fractions was conducted based on the protocol of Xie et al. (2024). Rat intestinal acetone powder was suspended in 0.12 M potassium phosphate buffer-I (*PPB-I*, with 1% NaCl, pH 6.8) at a ratio of 1:50 (*w/v*) to prepare the mammalian α-glucosidase enzyme solution. The suspension was sonicated at 50 Hz for 5 min, with an ice bath used to prevent a rapid increase in temperature. After centrifugation at 8000 × *g* for 15 min at 4 °C, the supernatant was collected as the enzyme solution. This solution should be freshly prepared and used immediately. Protein content was previously determined to be 3.37 ± 0.08 mg/mL by the Bradford assay, using bovine serum albumin (BSA) as the standard.

All procedures in this assay were performed on ice to maintain enzyme activity. In detail, 20 μL of each sample (at 0.5 mg/mL, 1 mg/mL, 2 mg/mL, and 3 mg/mL), 140 μL of 0.12 M *PPB-II* (no NaCl, pH 6.8), and 25 μL of the α-glucosidase enzyme solution were combined. The enzymatic reaction was initiated by adding 20 μL of a 12.5 mM aqueous solution of *p*-nitrophenyl-α-D-glucopyranoside (*p*-NPG). After a 60-min incubation at 37 °C, absorbance was measured at 410 nm. Acarbose (0–3 mg/mL) was used as a standard reference, with *PPB-I* as the solvent.

The potential effects of the sample solvent and the substrate were evaluated and controlled. The percentage inhibition of α-glucosidase was calculated using the following equation:

$$\%inhibition\ of\ \alpha-glucosidase = \frac{\left[1-\left(A_{Sample}-A_{Sample\ background}\right)\right]}{A_{Control}-A_{Control\ background}}\times 100\% \quad (1)$$

where:

- $A_{Sample}$ is the absorbance of the mixture containing the sample, enzyme, and *p*-NPG;
- $A_{Sample\ background}$ is the absorbance of the mixture containing the sample, the enzyme, and the *p*-NPG solvent (distilled water);
- $A_{Control}$ is the absorbance of the mixture containing sample solvent (100% methanol)/standard solvent (*PPB-I*), enzyme, and *p*-NPG;
- $A_{Control\ background}$ is the absorbance of the mixture containing the sample solvent/standard solvent, enzyme, and *p*-NPG solvent.

*2.4.2.2. α-Amylase inhibitory activity.* The α-amylase inhibitory assay followed the method described by Xie et al. (2024). Porcine pancreatic α-amylase was diluted to 250 units/mL with 20 mM sodium phosphate buffer-I (*SPB-I*, 7 mM NaCl, 1 mM $CaCl_2$, pH 6.8). *SPB-II* (20 mM, 7 mM NaCl, pH 6.8) was prepared for the substrate *p*-nitrophenyl-α-D-maltopentaoside (*p*-NPG6) solution (5 mg/mL).

In this assay, 20 μL of each sample (at concentrations of 0.5 mg/mL, 1 mg/mL, 2 mg/mL, and 3 mg/mL), 100 μL of *SPB-II*, and 50 μL of α-amylase solution were combined. All procedures were carried out on ice to preserve enzyme activity. The enzymatic reaction was triggered by adding 50 μL of *p*-NPG6 solution. After a 40-min incubation at 37 °C, absorbance was measured at 410 nm. Acarbose (0–3 mg/mL) was compared as a standard reference with *SPB-I* as the solvent.

The potential effects of the sample solvent and the substrate were evaluated and controlled. The percentage inhibition of α-amylase was calculated using the following equation:

$$\%inhibition\ of\ \alpha-amylase = \frac{\left[1-\left(A_{Sample}-A_{Sample\ background}\right)\right]}{A_{Control}-A_{Control\ background}}\times 100\% \quad (2)$$

where:

- $A_{Sample}$ is the absorbance of the mixture containing the sample, enzyme, and *p*-NPG6;
- $A_{Sample\ background}$ is the absorbance of the mixture containing the sample, enzyme, and *p*-NPG6 solvent (*SPB-II*);
- $A_{Control}$ is the absorbance of the mixture containing sample solvent (100% methanol)/standard solvent (*SPB-I*), enzyme, and *p*-NPG6;
- $A_{Control\ background}$ is the absorbance of the mixture containing the sample solvent/standard solvent, enzyme, and *p*-NPG6 solvent.

### 2.4.3. Anti-inflammatory activity

*2.4.3.1. Nitric oxide (NO) inhibitory activity.* The NO-inhibitory activity was assessed using a method adapted from Subbiah, Ebrahimi, Duan, et al. (2024). Sodium nitroprusside (5 mM) was dissolved in phosphate-buffered saline (PBS, pH 7.4) to generate NO. In this assay, 0.5 mL of each sample (at 0.5 mg/mL, 1 mg/mL, 2 mg/mL, and 3 mg/mL) and 2 mL of sodium nitroprusside solution (SNP) were mixed and incubated for 3 h at room temperature with light exposure, followed by adding 1 mL of Griess aqueous solution (1:25, *w/v*). After an additional 30-min incubation at room temperature, 300 μL of each mixture was added to the 96-well plates, and the absorbance was measured at 550 nm. Ascorbic acid (AA, 0–3 mg/mL) was used as a standard.

The percentage inhibition of NO was calculated using the following equation:

$$\%inhibition\ of\ nitric\ oxide\ (NO)\ radical = \frac{\left[1-\left(A_{Sample}-A_{Sample\ background}\right)\right]}{A_{Control}-A_{Control\ background}}\times 100\% \quad (3)$$

where:

- $A_{Sample}$ is the absorbance of the mixture containing the sample, SNP, and Griess solution;
- $A_{Sample\ background}$ is the absorbance of the mixture containing the sample, SNP, and Griess solution solvent (distilled water);
- $A_{Control}$ is the absorbance of the mixture containing sample solvent (100% methanol), SNP, and Griess solution;
- $A_{Control\ background}$ is the absorbance of the mixture containing the sample solvent, SNP, and Griess solution solvent.

*2.4.3.2. Bovine serum albumin (BSA) denaturation assay.* To assess the anti-inflammatory activity, 0.02 mL of each sample (at 0.5 mg/mL, 1 mg/mL, 2 mg/mL, and 3 mg/mL) was added to 0.2 mL of BSA aqueous solution (1%, *w/v*) and 4.78 mL of PBS buffer (pH 6.4). These mixtures were then incubated in a water bath (37 °C) for 15 min, followed by heating at 70 °C for 10 min. The samples were allowed to cool, and absorbance was measured at 660 nm. Diclofenac sodium (DIC, 0–3 mg/mL) was used as the standard for comparison. PBS buffer was used as a control in this experiment (Gunathilake et al., 2018).

The percentage of protein denaturation was determined using the following equation:

$$\%Protein\ denaturation = \left(\frac{A_{control}-A_{sample}}{A_{Control}}\right)\times 100\% \quad (4)$$

where:

- $A_{control}$ is the absorbance of PBS;
- $A_{sample}$ is the absorbance of samples.

### 2.5. Revident liquid chromatography/quadrupole time-of-flight mass spectrometry (Revident LC/Q-TOF MS)

Samples were injected into an Agilent Revident Q-TOF (Agilent

6520) coupled with Agilent 1290 Infinity II HPLC. Separation of samples was carried out on a Synergi™ Hydro-RP 80 Å, LC column (250 mm × 4.6 nm, 4 μm) (Phenomenex, Lane Cove, NSW, Australia) fitted with a C18 ODS guard column (Phenomenex, Torrance, CA). The gradient of 0.1% formic acid in water (*v/v*, A) and 0.1% formic acid in acetonitrile (*v/v*, B) at a constant flow rate of 0.8 mL/min was applied as follows: 0–4 min, 1–2% B; 4–10 min, 2–5% B; 10–50 min, 5–45% B; 50–52 min, 45–98% B; 52–54 min, 98% B; 54–56 min, 98–2% B. Injection volume was set as 1 μL. The LC stream was directed to waste for the first 4 min. Mass spectra were obtained in the *m/z* range 50–1500, with peak identification in both positive and negative ionization modes.

### 2.6. Statistical analysis and visualization

The experimental results were presented as mean values ± standard deviations (SD) from triplicate measurements. Where applicable, statistical analysis was performed using GraphPad Prism software (version 10.5.0). One-way/two-way analysis of variance (ANOVA) and Tukey's honestly significant difference (HSD) multiple-rank test was applied to assess significant differences among groups, with a significance threshold set at $p < 0.05$. Interactive Mantel test correlation heatmaps were generated using Chi Plot's heatmap tool (https://www.chiplot.online/).

## 3. Results and discussion

### 3.1. Phenolic compounds in seaweed-derived free fractions

#### 3.1.1. Quantification of phenolic compounds

Given the diverse chemical nature of phenolic compounds in brown seaweeds (e.g., phenolic acids, terpenoids, bromophenols, and phlorotannins) (Barzkar et al., 2024), a comprehensive assessment was conducted using four assays (TPC, TPhC, TFC, and TTC). This multi-method approach was chosen to mitigate methodological limitations and better capture the complex phenolic profile of the studied species.

The results of the four assays for the three species are presented in Fig. 1. The measured TPC values were highest in *F. vesiculosus* (21.61 ± 1.46 mg GAE/g), followed by *A. nodosum* (9.90 ± 0.62 mg GAE/g) and *E. radiata* (2.95 ± 0.23 mg GAE/g). A consistent and statistically significant trend (*F. vesiculosus* > *A. nodosum* > *E. radiata*) was observed for TPhC and TTC ($p < 0.05$), which closely mirrored the pattern observed in the TPC results. In stark contrast, TFC values were negligible across all species (consistently below 0.3 mg QE/g). These values were orders of magnitude lower than those typically reported for phenolic-rich plant extracts and fell below the range required for meaningful discrimination among species under the current analytical conditions. This primarily reflects a methodological constraint rather than a true absence of flavonoid-like structures. The aluminum chloride colorimetric assay is inherently structure-dependent, relying on metal chelation by specific functional groups (e.g., 3- or 5-hydroxyl groups in conjugation with a 4-keto group) (Nicolescu et al., 2025), and may therefore systematically underestimate flavonoid-like constituents lacking these canonical motifs, particularly in structurally diverse seaweed matrices. This interpretation is supported by LC-MS characterization, which tentatively identified 21, 13, and 20 flavonoid-annotated compounds in the free fractions of *E. radiata*, *F. vesiculosus*, and *A. nodosum*, respectively. These findings demonstrate that flavonoid-like chemical richness is present but not captured by the colorimetric method. All subsequent TFC data in this study should be interpreted in light of this constraint.

Numerous studies have shown that the synthesis of secondary metabolites (e.g., phenolics) is strongly influenced by environmental stressors, such as UV radiation and desiccation, which make their abundance a reliable indicator of stress adaptation across species (Wang et al., 2022). This ecological framework helps explain the observed pattern. *F. vesiculosus* typically grows in the mid-tide zone of high-salinity waters (Catarino et al., 2018) and is therefore hypothesized to possess high baseline levels of secondary metabolites such as phenolics to defend against environmental stresses, similar to another mid-intertidal species, *A. nodosum* (Cervin et al., 2004). Literature reports confirm these high phenolic contents in these species, with TPhC values reaching 140 mg/g (14% DW) in *A. nodosum* and 122 mg/g (12.2% DW) in *Fucus* sp. (Holdt & Kraan, 2011). Furthermore, the predominance of phlorotannins in these extracts is supported by studies showing that PVPP, a polymer that selectively binds phenolics, can remove 60–90% of the extractable material from *A. nodosum* (Toth & Pavia, 2001).

In contrast, *E. radiata* inhabits subtidal rocky reefs, a relatively stable underwater environment characterized by reduced UV exposure and the absence of desiccation stress (Poloczanska et al., 2009). Such environmental conditions are generally associated with lower oxidative and herbivory pressures, which may contribute to reduced constitutive phenolic production. Although direct comparative studies among these species are limited, lower levels of extractable phenolics have also been reported in other subtidal genera, such as *Laminaria*, supporting a habitat-related explanation. For example, the sublittoral macroalga *Laminaria hyperborea* showed TPC values of approximately 1.5 mg GAE/g (O'Sullivan et al., 2011), and *Laminaria digitata* ranged from 0.0022 to 0.324 mg GAE/g (Farvin & Jacobsen, 2013; Heffernan et al., 2014). In contrast, the intertidal species *F. vesiculosus*, which experiences greater environmental stress, showed higher TPC values ranging from 2.5 to 12.0 mg GAE/g (Farvin & Jacobsen, 2013; O'Sullivan et al., 2011). These differences likely reflect ecological and habitat-related variation in phenolic investment rather than methodological discrepancies.

Flavonoid contents were consistently low across all three species (0–0.3 mg QE/g), in line with previous findings for *E. radiata* (~0.2 mg QE/g) reported by Subbiah, Ebrahimi, Agar, et al. (2024). However, this differs markedly from the results of Obluchinskaya et al. (2022), who reported TFC values ranging from 15.6 to 26.4 mg QE/g in *F. vesiculosus*. Such discrepancies could be explained by variations in geographical

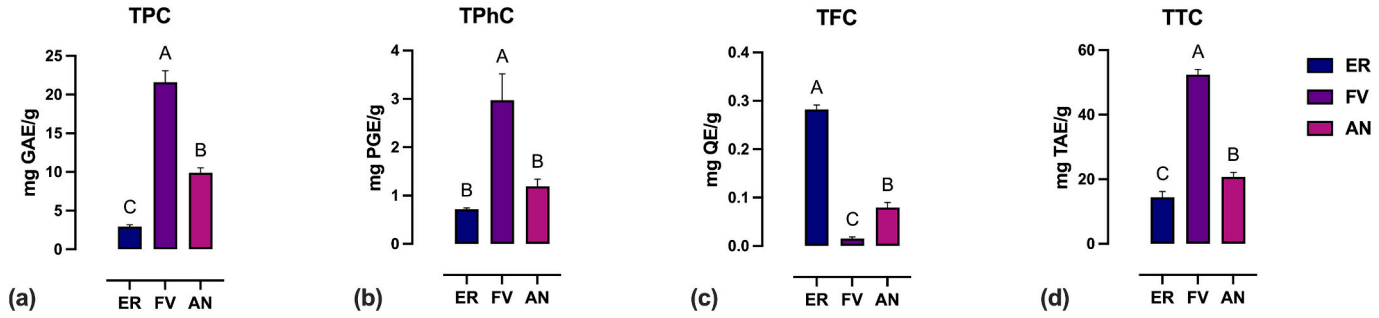


**Fig. 1. Quantification of phenolic compounds in seaweed-derived free fractions.** ER, *Ecklonia radiata*; FV, *Fucus vesiculosus*; AN, *Ascophyllum nodosum*; (a) TPC, total phenolic content; (b) TPhC, total phlorotannin content; (c) TFC, total flavonoid content; (d) TTC, total tannin content; GAE, gallic acid equivalent; PGE, phloroglucinol equivalent; QE, quercetin equivalent; TAE, tannic acid equivalent. Different uppercase letters (A-C) refer to statistically significant differences ($p < 0.05$).

origin, seasonal timing, or reproductive stage. Nonetheless, given the overall low flavonoid levels observed in this study, comparisons based solely on TFC values may not provide robust insights into interspecific differences as discussed above.

### 3.1.2. Biological activities of free fractions

Antioxidant, anti-diabetic, and anti-inflammatory biological potentials of seaweed-derived free phenolic fractions were assessed through in vitro assays, with results shown in Fig. 2. For completeness, calculated potency indices, including IC50 and RC1.0 (as defined in **Section 2.4.1**), are provided in the **SI. Table. S1** to facilitate quantitative comparison.

In general, *E. radiata* exhibited the lowest antioxidant activity and *F. vesiculosus* the highest (Fig. 2 **(a-c)**). The differences aligned with the trend in phenolic content, with higher phenolic content associated with greater activity. In both the DPPH and FRAP assays, a typical concentration-dependent response was observed, particularly in *E. radiata* and *A. nodosum*. This response reflects enhanced electron-donating capacity and free radical scavenging activity, mechanisms by which these extracts mitigate oxidative stress (Chandimali et al., 2025). As shown in Fig. 2(a), the DPPH radical scavenging activity was concentration dependent. At 3 mg/mL, *A. nodosum* exhibited the highest activity (134.17 ± 0.75 μg Trolox/mL), which was significantly greater ($p < 0.05$) than that of *F. vesiculosus* (130.63 ± 0.74 μg Trolox/mL) and *E. radiata* (86.34 ± 0.10 μg Trolox/mL). The FRAP assay showed a similar trend (Fig. 2(b)), with *F. vesiculosus* exhibiting the greatest ferric-reducing power at the highest concentration (453.43 ± 4.86 μg Trolox/mL). However, DPPH values of *F. vesiculosus* reflected a weaker concentration-dependent response, with significant differences ($p < 0.05$) observed only between the highest (130.63 ± 0.74 μg Trolox/mL at 3 mg/mL) and the lowest (123.12 ± 0.44 μg Trolox/mL at 0.5 mg/mL) concentrations, which indicated a plateau phase possibly due to saturation of the reaction system. A similarly flat trend was reported by Lukova et al. (2024) for the alga *Ericaria crinite*, which showed no significant increase ($p > 0.05$) in DPPH activity as the concentration increased from 1.75 to 2.5 mg/mL. The limited dynamic response to increasing concentrations is consistent with saturation-driven nonlinearity commonly in high-activity samples (Brand-Williams et al., 1995; Kedare & Singh, 2011). Notably, the FICA results showed limited variation and no clear concentration-dependent pattern, with values ranging from 8.38 ± 0.55 to 19.05 ± 1.09 μg EDTA/mL. The inconsistency, in contrast to the more concentration-responsive results observed in the other two antioxidant assays, suggests that phenolic content does not primarily govern iron chelation capacity. Instead, it is likely influenced by the presence of specific functional groups that bind metal ions. Previous studies have highlighted that effective metal chelation by phenolics depends on structural features such as a 4-keto group in conjugation with 3- and/or 5-hydroxyl groups, or ortho-dihydroxy (catechol) arrangements at the 3′,4′, or 7,8 positions in the B-ring of flavonoids (Khokhar & Owusu Apenten, 2003). The relatively low flavonoid content detected in the samples may also contribute to the weak and non-distinctive FICA response observed. Moreover, phenolic compounds containing only a single hydroxyl group also lack sufficient

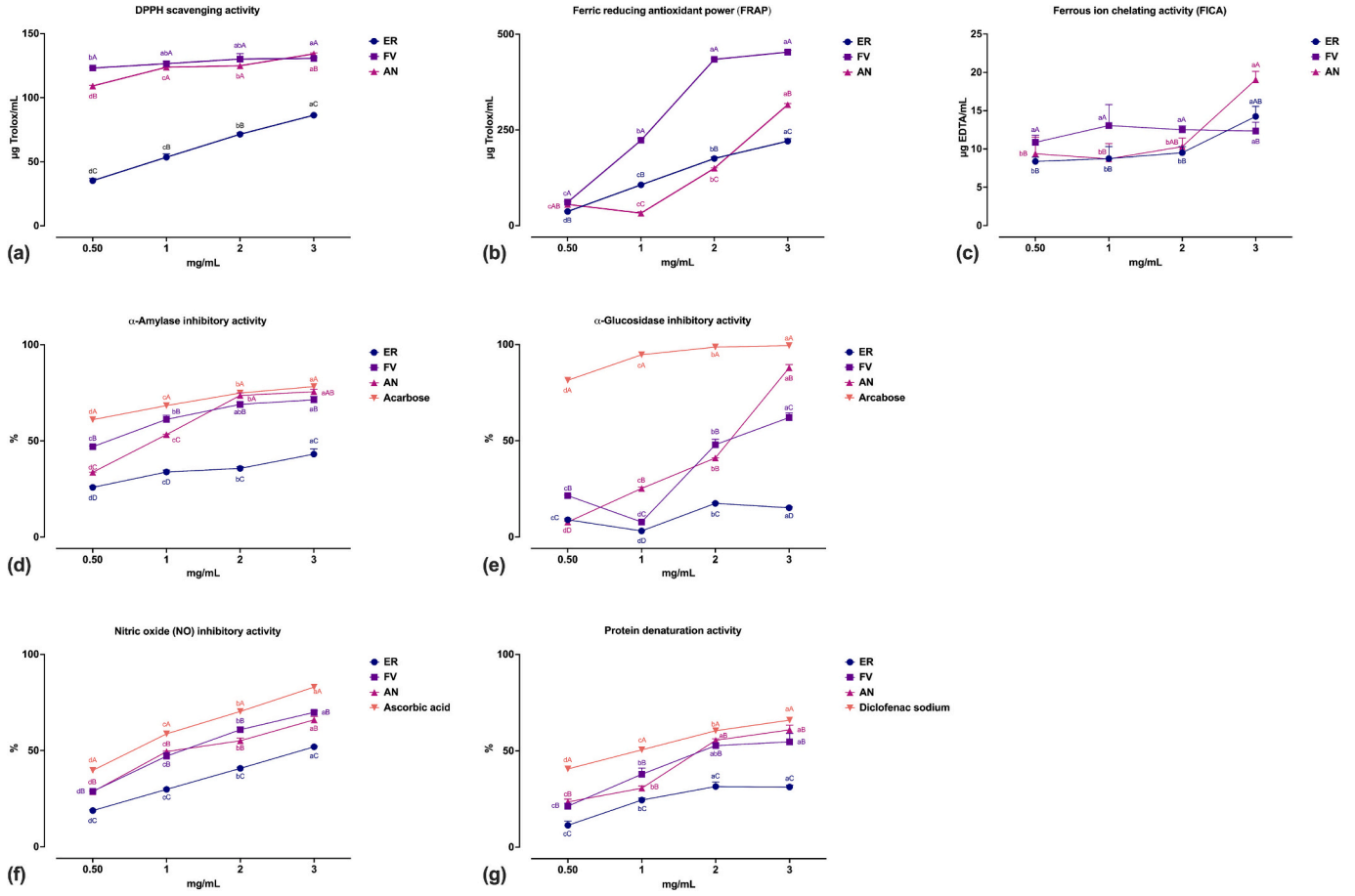


**Fig. 2. Estimation of biological potential of phenolic compounds in seaweed-derived free fractions.** ER, *Ecklonia radiata*; FV, *Fucus vesiculosus*; AN, *Ascophyllum nodosum*. (a) DPPH radical scavenging activity (μg Trolox/mL), (b) ferric reducing antioxidant power (μg Trolox/mL), (c) ferrous ion chelating activity (μg EDTA/mL), (d) α-amylase inhibitory activity (%), (e) α-glucosidase inhibitory activity, (f) nitric oxide (NO) inhibitory activity (%), (g) protein denaturation ability (%). Values are mean ± SD (n = 3). Different uppercase letters (A-D) indicate significant differences ($p < 0.05$) between different seaweed species at the same concentration, while lowercase letters (a-d) denote significant differences ($p < 0.05$) among different concentrations within the same seaweed species.

structural complexity to chelate transition metals effectively (Zhou et al., 2006).

Inhibition of α-amylase and α-glucosidase is a widely accepted in vitro strategy to evaluate the potential anti-diabetic activity of natural compounds, due to the central roles of these enzymes in carbohydrate digestion and postprandial glycemic regulation (Ratananikom et al., 2024). The inhibitory activities of the seaweed extracts are presented in Fig. 2 **(d-e)**, with acarbose used as a positive control ($IC_{50}$ for α-amylase: 0.1917 mg/mL; for α-glucosidase: 0.2426 mg/mL; see **SI. Fig. S1 (a-b)**). At a concentration of 1 mg/mL, the extracts inhibited α-amylase activity by 33.83 ± 1.00% to 61.18 ± 2.09% and α-glucosidase by 3.15 ± 0.30% to 25.23 ± 0.74%, which was significantly weaker ($p < 0.05$) than that achieved by an equivalent concentration of acarbose (68.35% and 94.67%, respectively). Although a consistent inhibition trend (*A. nodosum* ≥ *F. vesiculosus* > *E. radiata*) was observed in both assays, marked differences emerged among the two enzymes and among the species. Notably, seaweed extracts showed a limited concentration-dependent effect on α-glucosidase, suggesting a more selective inhibition profile. However, contrasting results have been reported. For example, flavonols isolated from *Stenochlaena palustris* showed a higher affinity for α-glucosidase than for α-amylase (Hendra et al., 2024). The authors highlighted structural determinants of enzyme selectivity, including the hydroxylation pattern of the B-ring, glycosylation at the C3-OH, and the presence of a C2═C3 double bond in the C-ring. Other studies proposed that α-amylase allows more effective binding to high-molecular-weight (HWM) polyphenols. For instance, Lee et al. (2007) reported that polymerized proanthocyanidins significantly enhanced α-amylase inhibition (53.9 ± 1.2%, $p < 0.001$) compared to oligomers (4.6 ± 4.0%). Conversely, α-glucosidase inhibition followed the opposite trend, with oligomers (97.4 ± 0.1%) being more potent than polymers (74.0 ± 1.0%). The narrower and more restrictive binding pocket of α-glucosidase may hinder interactions with bulky or highly hydroxylated molecules. Supporting this, Akkarachiyasit et al. (2010) found that among cyanidin derivatives, cyanidin-3-galactoside ($IC_{50}$ = 0.5 mM) exhibited potent α-glucosidase inhibition, whereas cyanidin-3,5-diglucoside ($IC_{50}$ > 2.0 mM) was inactive, which further emphasized the importance of molecular size and structure in enzyme targeting.

The NO and BSA denaturation assays are established in vitro methods to assess anti-inflammatory activity, as they simulate key mechanisms of inflammation, including oxidative stress and protein destabilization. Ascorbic acid and diclofenac sodium were used as standard references, shown in **SI. Fig. S1 (c-d)**. According to Fig. 2 **(f-g),** all three species showed a consistent concentration-dependent trend, with *F. vesiculosus* ≥ *A. nodosum* > *E. radiata*. The activities of *F. vesiculosus* and *A. nodosum* were closely aligned in both assays, suggesting that their bioactive components may exert similar protective and radical-scavenging effects under the tested conditions. Although *E. radiata* consistently showed low NO inhibition activity across all concentrations, within a narrow concentration range (0.5–3 mg/mL), it produced inhibition levels (18.82 ± 0.42% to 51.96 ± 0.25%) that were comparable to those reported in previous studies for *Enteromorpha linza*, *Porphyra tenera*, *Sargassum fusiforme*, and *Undaria pinnatifida*, which showed inhibition ranging from 6.88 ± 1.7% to 55.41 ± 2.5% over a broader concentration range (0.1–8 mg/mL). The comparable inhibition levels achieved at lower maximum concentrations may reflect differences in phytochemical composition, particularly the abundance or accessibility of specific polyphenols. In addition, the overall BSA denaturation inhibitory activities of all tested samples (11.39 ± 2.18% to 60.89 ± 2.41%) fell within a relatively narrow range. Comparable inhibition levels have been reported for *F. vesiculosus* extracts prepared with acetone, ethanol, or methanol (~20–60% at 125–1000 μg/mL, using ibuprofen as a standard), despite being tested at lower concentrations (Rossi et al., 2024). By contrast, ethanol extracts of *Dictyota implexa* showed much more vigorous activity, ranging from 45.38 ± 0.84% to 103.64 ± 1.28% at concentrations of only 5–100 μg/mL (Trang Thuy & Men, 2025).

### 3.2. Phenolic compounds in seaweed-derived bound fractions

#### 3.2.1. Quantification of phenolic compounds

An interesting species-specific pattern was observed in the phenolic distribution of the three brown algae. *F. vesiculosus* and *A. nodosum* were predominantly characterized by free phenolic compounds, with only trace amounts detected in the bound fraction. In contrast, *E. radiata* exhibited the opposite trend, with a markedly higher proportion of phenolics present in the bound form (Fig. 3). This interspecific difference is consistent with previous findings reporting a low bound-to-free TPhC ratio (0.11) in *F. vesiculosus*, which confirmed the generally limited contribution of bound phenolics in this species (Koivikko et al., 2005). Importantly, this free-dominant versus bound-dominant distribution pattern was consistently reflected across the TPC, TPhC, and TTC assays, suggesting that the pH-mediated hydrolysis treatments reproducibly captured species-specific phenolic partitioning rather than generating assay-dependent artifacts.

In terms of TPC values, the bound phenolics in all three species were suppressed under acidic conditions but markedly elevated under alkaline conditions, following the overall trend of pH 13 > pH 10 > pH 1 ≈ pH 4. Quantitatively, *E. radiata* achieved 12.87 ± 0.64 mg GAE/g at pH 13, approximately 2.62-fold higher than at pH 4. Although *F. vesiculosus* and *A. nodosum* exhibited very low yields under acidic conditions (0.30 ± 0.02 mg GAE/g and 0.60 ± 0.12 mg GAE/g, respectively), their levels increased significantly by 10.89-fold and 9.56-fold ($p < 0.05$), respectively, under strongly alkaline treatment. The substantially higher bound phenolic levels in *E. radiata* suggest either a naturally greater reservoir of bound phenolics or weaker interactions between phenolics and the cell wall matrix. When comparing acidic (pH 1 and 4) and alkaline (pH 10 and 13) conditions, the calculated base/acid ratios for the three algae were 1.92, 7.06, and 5.31, which indicated strong sensitivity to alkalinity, especially in *F. vesiculosus* and *A. nodosum*. Under mildly acidic conditions (pH 4), yields were consistently lowest. A similar trend was observed in *Saccharina latissima*, where stronger acidification facilitated the release of biomass components, such as mannitol and minerals, whereas weaker acidification preserved greater structural integrity of the cell wall matrix (Krook et al., 2024). Polyphenols may exhibit similar release behavior. One possible explanation for the higher TPC values under strongly alkaline conditions is the enhanced solubility of phenolic compounds. Given that the pKa of most phenolics ranges between approximately 9 and 11 (Sobiesiak, 2017), their hydroxyl groups (–OH) are largely deprotonated into phenolate anions ($–O^-$) at pH values above 12. These negatively charged species exhibit strong ion-dipole interactions with water molecules, thereby enhancing their solubility in aqueous solutions. In addition to ionizing hydroxyl groups, strong alkaline conditions can disrupt secondary interactions within seaweed matrices, such as inter-polysaccharide interactions (e.g., alginate, fucoidan, agar, and carrageenan) and phenolic self-aggregation via hydrogen bonding, hydrophobic forces, and van der Waals interactions (Lee et al., 2025). Alkalinity can also cleave ester or ether linkages (if present). Saponification of ester bonds under intense alkaline conditions (Kusmiyati et al., 2023) compromises cell wall integrity, leading to swelling or partial dissolution. This structural disruption reduces the cell wall's barrier function and facilitates solvent penetration, thereby enhancing the diffusion of intracellular or wall-bound phenolics. By contrast, weakly alkaline conditions (e.g., pH 10) provide insufficient hydroxide ion ($OH^-$) concentration to fully deprotonate phenolic hydroxyl groups. Consequently, improvements in solubility and matrix disruption remain limited. In acidic environments, hydroxyl groups remain protonated (–OH), decreasing hydrophilicity and lowering solubility in aqueous systems.

TTC exhibited a different pH-dependent pattern, with the maximum value observed at pH 10 (36.28 ± 0.38 mg TAE/g in *E. radiata*). The results indicate that low alkalinity enhances the release of tannin-like compounds compared with other conditions. Similar observations have been reported in single-factor experiments, in which non-

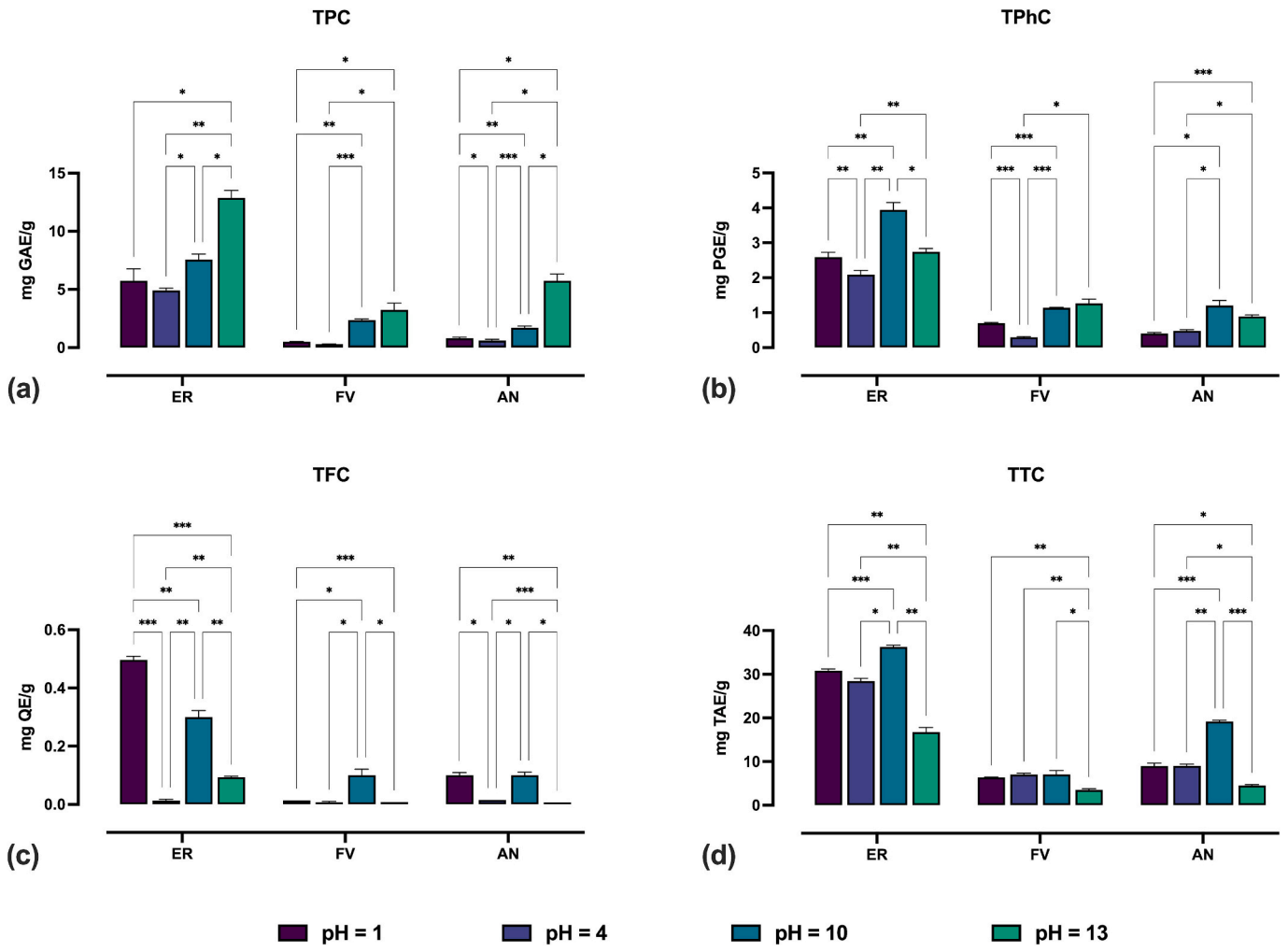


**Fig. 3. Release of bound phenolic compounds through pH-mediated hydrolysis.** ER, *Ecklonia radiata*; FV, *Fucus vesiculosus*; AN, *Ascophyllum nodosum*. (a) TPC, total phenolic content; (b) TPhC, total phlorotannin content; (c) TFC, total flavonoid content; (d) TTC, total tannin content; GAE, gallic acid equivalent; PGE, phloroglucinol equivalent; QE, quercetin equivalent; TAE, tannic acid equivalent. Values are mean ± SD (n = 3). Asterisks indicate significant differences among pH treatments within the same seaweed species (*$p < 0.05$, **$p < 0.01$, ***$p < 0.001$). Non-significant comparisons are not shown.

extractable polyphenols (i.e., hydrolysable tannins and proanthocyanidins associated with dietary fiber and/or protein) yielded the highest yields at 0.1 mol/L NaOH but declined at higher concentrations (Cheng et al., 2014). Although no mechanistic explanation was provided in that study, the data are consistent with the interpretation that stronger alkaline conditions induce partial degradation or structural alteration of tannins, thereby offsetting the benefits of enhanced bond cleavage. Comparison with acidic treatments further supports the superiority of alkaline hydrolysis. Mild alkaline hydrolysis efficiently cleaved the ester linkage, which liberated bound tannins from cell wall matrices, and produced significantly higher yields (54.33 mg/g) than acid hydrolysis (27.25 mg/g) (Cheng et al., 2014). In contrast, strongly or moderately acidic conditions (pH 1–4) released substantially lower amounts of tannins. Acidic hydrolysis tends to promote precipitation, especially in the presence of proteins (Bone & Mills, 2013).

In brown seaweeds, tannins are primarily composed of phlorotannins (Alloyarova et al., 2024), a feature that necessitates special consideration for their extraction. The extraction efficiency for TPhC showed a trend similar to that of TTC, with the highest yield (3.94 ± 0.21 mg PGE/g) obtained at pH 10, which was significantly higher than those at other pH values ($p < 0.05$). These findings can be attributed to the structural nature of phlorotannins, which are polymers of phloroglucinol interconnected by aryl ether, diaryl ether, or C–C bonds (Heffernan et al., 2015). Among these linkages, ether bonds are specifically susceptible to nucleophilic attack and thus vulnerable to base-catalyzed hydrolysis (Manohar et al., 2025; Pufky-Heinrich et al., 2018). Therefore, the mild alkaline condition (pH 10) possibly increases the solubility of phlorotannins by partially cleaving these bonds without causing widespread destruction. In contrast, stronger alkaline conditions may induce extensive depolymerization and degradation of phloroglucinol subunits (cf. Osawa and Walsh (1993), for an analogous case involving phenolic acids), ultimately leading to reduced detectable TPhC. Acidic conditions exerted complex effects on phlorotannin yield. Contrary to the expected trend of degradation in a strongly acidic environment, our data showed that TPhC values under strong acidic hydrolysis were higher than those under weak acidic conditions. This counterintuitive result arises from a balance between degradation and extraction efficiency. While strong acid undoubtedly promotes the hydrolysis of labile bonds within phlorotannins, it is also far more effective than weak acidic conditions at disrupting the intricate polysaccharide-protein matrix of the brown seaweed cell wall. This aggressive disruption liberates a significant fraction of bound or encapsulated phlorotannins that would otherwise remain inaccessible under milder extraction conditions. Consequently, even though some degradation occurs, the net yield is higher because of the greatly improved release of these compounds into the solvent.

Theoretically, under moderate alkaline conditions, phenolic hydroxyl groups of flavonoid aglycones can ionize to form negatively

charged –O⁻ forms, which increase their solubility in water and enhance their detectability. This rationale may explain the apparent trend of marginally higher TFC values observed at pH 10 compared to other conditions (except for *E. radiata*).

### 3.2.2. Biological activities of bound fractions

The biological activities of seaweed-bound phenolic fractions were also evaluated across three aspects, as shown in Table 1. Calculated potency indices are provided in **SI. Table S2.**

The antioxidant potential of the bound fractions was assessed using

**Table 1**
Estimation of biological potential of phenolic compounds in seaweed-derived free fractions.

| Concentrations | *Ecklonia radiata* | | | | *Fucus vesiculosus* | | | | *Ascophyllum nodosum* | | | |
|---|---|---|---|---|---|---|---|---|---|---|---|---|
| | pH = 1 | pH = 4 | pH = 10 | pH = 13 | pH = 1 | pH = 4 | pH = 10 | pH = 13 | pH = 1 | pH = 4 | pH = 10 | pH = 13 |
| ***DPPH scavenging activity (μg Trolox/mL)*** | | | | | | | | | | | | |
| **0.5 mg/mL** | 75.88 ± 0.65 $^{dB}$ | 73.72 ± 1.67 $^{dBC}$ | 72.48 ± 0.64 $^{dC}$ | 83.55 ± 3.69 $^{dA}$ | 17.99 ± 1.70 $^{cH}$ | 28.47 ± 0.47 $^{dG}$ | 27.65 ± 0.79 $^{dG}$ | 28.62 ± 2.40 $^{dG}$ | 44.97 ± 2.14 $^{dD}$ | 36.69 ± 0.23 $^{cE}$ | 31.88 ± 1.43 $^{dF}$ | 44.45 ± 0.66 $^{dD}$ |
| **1 mg/mL** | 96.95 ± 2.16 $^{cC}$ | 96.35 ± 1.19 $^{cC}$ | 101.21 ± 2.33 $^{cB}$ | 112.99 ± 1.28 $^{cA}$ | 26.06 ± 0.71 $^{bH}$ | 39.74 ± 0.84 $^{cF}$ | 39.24 ± 1.13 $^{cF}$ | 39.89 ± 1.68 $^{cF}$ | 52.21 ± 0.29 $^{cE}$ | 35.04 ± 2.68 $^{cG}$ | 35.95 ± 0.68 $^{cG}$ | 67.83 ± 0.49 $^{cD}$ |
| **2 mg/mL** | 121.27 ± 1.74 $^{bC}$ | 123.04 ± 0.93 $^{bBC}$ | 125.13 ± 1.72 $^{bB}$ | 145.22 ± 1.72 $^{bA}$ | 35.02 ± 1.08 $^{aI}$ | 80.42 ± 0.91 $^{bF}$ | 67.21 ± 0.53 $^{bG}$ | 79.10 ± 1.12 $^{bF}$ | 84.04 ± 2.35 $^{bE}$ | 63.68 ± 0.81 $^{bH}$ | 62.01 ± 1.70 $^{bH}$ | 110.03 ± 1.10 $^{bD}$ |
| **3 mg/mL** | 143.54 ± 0.43 $^{aB}$ | 142.31 ± 1.67 $^{aB}$ | 144.01 ± 1.57 $^{aB}$ | 168.21 ± 0.70 $^{aA}$ | 27.99 ± 1.86 $^{bH}$ | 98.57 ± 1.34 $^{aE}$ | 82.04 ± 1.98 $^{aF}$ | 101.90 ± 1.96 $^{aD}$ | 97.74 ± 2.68 $^{aE}$ | 79.94 ± 2.28 $^{aFG}$ | 78.78 ± 2.73 $^{aG}$ | 119.35 ± 0.75 $^{aC}$ |
| ***Ferric reducing antioxidant power (FRAP) (μg Trolox/mL)*** | | | | | | | | | | | | |
| **0.5 mg/mL** | 48.36 ± 3.68 $^{dAB}$ | 50.43 ± 3.47 $^{dA}$ | 46.76 ± 2.93 $^{dB}$ | 41.66 ± 3.26 $^{dC}$ | 4.19 ± 0.36 $^{cGH}$ | 9.31 ± 2.11 $^{cEF}$ | 6.46 ± 0.36 $^{dFG}$ | 6.43 ± 0.22 $^{dFG}$ | 11.38 ± 1.11 $^{cDE}$ | 4.12 ± 0.70 $^{dGH}$ | 2.77 ± 0.63 $^{dH}$ | 12.99 ± 1.95 $^{dD}$ |
| **1 mg/mL** | 96.11 ± 8.59 $^{cA}$ | 102.09 ± 6.12 $^{cA}$ | 88.79 ± 3.10 $^{cB}$ | 96.58 ± 5.14 $^{cA}$ | 4.43 ± 0.23 $^{cF}$ | 35.01 ± 2.25 $^{bC}$ | 24.47 ± 1.57 $^{cD}$ | 33.92 ± 3.08 $^{cC}$ | 10.09 ± 0.88 $^{cEF}$ | 15.14 ± 0.73 $^{cE}$ | 6.64 ± 1.91 $^{cF}$ | 31.38 ± 0.57 $^{cC}$ |
| **2 mg/mL** | 213.33 ± 12.16 $^{bB}$ | 213.21 ± 11.27 $^{bB}$ | 222.52 ± 14.77 $^{bB}$ | 268.55 ± 6.95 $^{bA}$ | 23.38 ± 0.49 $^{bF}$ | 81.93 ± 3.01 $^{aCD}$ | 76.20 ± 0.72 $^{bD}$ | 89.36 ± 2.83 $^{bC}$ | 42.14 ± 1.36 $^{bE}$ | 28.09 ± 1.19 $^{bF}$ | 33.07 ± 0.86 $^{bEF}$ | 90.47 ± 3.13 $^{bC}$ |
| **3 mg/mL** | 289.95 ± 12.94 $^{aB}$ | 291.02 ± 13.13 $^{aB}$ | 284.73 ± 6.73 $^{aB}$ | 349.84 ± 12.94 $^{aA}$ | 24.74 ± 0.65 $^{aG}$ | 83.67 ± 1.47 $^{aE}$ | 84.86 ± 0.49 $^{aE}$ | 101.56 ± 2.27 $^{aD}$ | 77.43 ± 1.09 $^{aE}$ | 46.67 ± 1.74 $^{aF}$ | 44.57 ± 1.37 $^{aF}$ | 132.85 ± 6.81 $^{aC}$ |
| ***Ferrous ion chelating activity (FICA) (μg EDTA/mL)*** | | | | | | | | | | | | |
| **0.5 mg/mL** | 9.11 ± 0.55 $^{bCDE}$ | 8.93 ± 1.04 $^{bDE}$ | 8.94 ± 0.22 $^{bcDE}$ | 10.94 ± 0.91 $^{bABC}$ | 7.42 ± 0.42 $^{dE}$ | 10.91 ± 1.84 $^{dABC}$ | 10.99 ± 0.30 $^{dABC}$ | 11.39 ± 0.81 $^{dAB}$ | 10.51 ± 0.89 $^{dBCD}$ | 12.68 ± 1.86 $^{dA}$ | 12.14 ± 1.70 $^{dAB}$ | 11.57 ± 1.14 $^{dAB}$ |
| **1 mg/mL** | 9.74 ± 0.22 $^{bDE}$ | 10.18 ± 1.56 $^{bDE}$ | 8.62 ± 0.45 $^{cE}$ | 12.21 ± 2.20 $^{bD}$ | 12.24 ± 0.27 $^{cD}$ | 19.88 ± 0.16 $^{cAB}$ | 16.61 ± 1.17 $^{cC}$ | 18.01 ± 3.39 $^{cBC}$ | 22.34 ± 2.37 $^{cA}$ | 20.75 ± 1.14 $^{cAB}$ | 22.69 ± 1.56 $^{cA}$ | 20.27 ± 3.48 $^{cAB}$ |
| **2 mg/mL** | 9.30 ± 0.26 $^{bG}$ | 8.78 ± 1.00 $^{bG}$ | 9.90 ± 0.76 $^{bG}$ | 12.57 ± 0.96 $^{bF}$ | 27.05 ± 0.27 $^{bE}$ | 35.17 ± 1.42 $^{bC}$ | 39.24 ± 1.83 $^{bB}$ | 41.21 ± 1.09 $^{bA}$ | 38.49 ± 0.84 $^{bB}$ | 30.19 ± 0.31 $^{bD}$ | 29.44 ± 0.35 $^{bD}$ | 34.11 ± 0.87 $^{bC}$ |
| **3 mg/mL** | 18.31 ± 0.67 $^{aE}$ | 18.38 ± 0.61 $^{aE}$ | 15.1 ± 0.61 $^{aF}$ | 20.56 ± 0.94 $^{aD}$ | 46.94 ± 0.67 $^{aC}$ | 51.59 ± 0.36 $^{aA}$ | 49.74 ± 1.00 $^{aB}$ | 51.68 ± 0.27 $^{aA}$ | 52.38 ± 0.16 $^{aA}$ | 52.18 ± 0.23 $^{aA}$ | 51.35 ± 1.10 $^{aA}$ | 49.72 ± 0.15 $^{aB}$ |
| ***α-Amylase inhibitory activity (%)*** | | | | | | | | | | | | |
| **0.5 mg/mL** | 3.39 ± 0.20 $^{dF}$ | 8.50 ± 0.46 $^{dC}$ | 12.93 ± 0.98 $^{dB}$ | 14.95 ± 0.27 $^{dA}$ | – | – | – | – | 3.25 ± 0.59 $^{cF}$ | 5.41 ± 0.45 $^{cE}$ | 0.86 ± 0.88 $^{cG}$ | 6.80 ± 0.99 $^{cD}$ |
| **1 mg/mL** | 15.16 ± 1.24 $^{cD}$ | 17.93 ± 1.25 $^{cC}$ | 22.91 ± 1.92 $^{cB}$ | 27.94 ± 1.43 $^{cA}$ | – | – | – | – | 5.22 ± 0.54 $^{bF}$ | 4.31 ± 0.32 $^{cF}$ | 5.66 ± 0.19 $^{bF}$ | 9.17 ± 0.64 $^{bE}$ |
| **2 mg/mL** | 45.96 ± 0.44 $^{bC}$ | 41.10 ± 0.25 $^{bD}$ | 50.37 ± 0.81 $^{bB}$ | 52.78 ± 1.63 $^{bA}$ | – | 1.72 ± 0.08 $^{bIJ}$ | 0.58 ± 0.21 $^{bJK}$ | 3.11 ± 0.24 $^{bHI}$ | 4.54 ± 1.39 $^{bcH}$ | 8.47 ± 1.39 $^{bF}$ | 6.92 ± 1.13 $^{bG}$ | 10.78 ± 0.69 $^{bE}$ |
| **3 mg/mL** | 78.08 ± 0.39 $^{aB}$ | 67.07 ± 3.45 $^{aC}$ | 80.61 ± 2.40 $^{aAB}$ | 82.71 ± 0.85 $^{aA}$ | 9.78 ± 0.61 $^{aHI}$ | 8.43 ± 2.87 $^{aI}$ | 10.29 ± 1.62 $^{aGHI}$ | 12.66 ± 1.02 $^{aFG}$ | 12.39 ± 0.70 $^{aFGH}$ | 14.01 ± 0.70 $^{aEF}$ | 15.8 ± 0.87 $^{aE}$ | 31.80 ± 1.25 $^{aD}$ |
| ***α-Glucosidase inhibitory activity (%)*** | | | | | | | | | | | | |
| **0.5 mg/mL** | 9.85 ± 0.13 $^{cD}$ | 18.55 ± 0.20 $^{aB}$ | 15.17 ± 0.06 $^{aC}$ | 19.42 ± 0.09 $^{aA}$ | 6.51 ± 0.24 $^{aG}$ | 9.17 ± 0.22 $^{aE}$ | 8.66 ± 0.07 $^{aF}$ | 14.83 ± 0.71 $^{aC}$ | – | – | – | 2.68 ± 0.11 $^{dH}$ |
| **1 mg/mL** | 5.62 ± 0.41 $^{dB}$ | – | 0.50 ± 0.25 $^{dE}$ | 1.98 ± 0.44 $^{dD}$ | 6.21 ± 0.39 $^{aA}$ | – | – | 0.51 ± 0.07 $^{bE}$ | – | – | – | 4.17 ± 0.87 $^{cC}$ |
| **2 mg/mL** | 17.89 ± 0.09 $^{aA}$ | 15.07 ± 0.19 $^{bB}$ | 10.39 ± 0.41 $^{cD}$ | 12.88 ± 0.51 $^{bC}$ | – | – | – | – | – | – | – | 9.62 ± 0.27 $^{bE}$ |
| **3 mg/mL** | 11.25 ± 0.48 $^{bB}$ | 9.28 ± 0.17 $^{cC}$ | 11.51 ± 0.33 $^{bB}$ | 8.05 ± 0.22 $^{cD}$ | 0.95 ± 0.66 $^{bF}$ | – | – | – | – | 4.78 ± 0.29 $^{aE}$ | 8.15 ± 0.35 $^{aD}$ | 12.2 ± 0.53 $^{aA}$ |
| ***Nitric oxide (NO) inhibitory activity (%)*** | | | | | | | | | | | | |
| **0.5 mg/mL** | 31.51 ± 1.38 $^{cAB}$ | 34.09 ± 0.52 $^{dA}$ | 30.80 ± 0.47 $^{dB}$ | 30.97 ± 0.22 $^{dB}$ | 4.76 ± 2.65 $^{cEF}$ | 8.49 ± 2.24 $^{cD}$ | 9.08 ± 2.60 $^{cD}$ | 4.03 ± 1.15 $^{dF}$ | 6.86 ± 0.51 $^{dDE}$ | 3.08 ± 1.76 $^{cF}$ | 3.58 ± 1.00 $^{cF}$ | 15.54 ± 2.32 $^{dC}$ |
| **1 mg/mL** | 60.61 ± 0.45 $^{bB}$ | 62.45 ± 0.89 $^{cAB}$ | 62.26 ± 0.37 $^{cAB}$ | 63.39 ± 0.34 $^{cA}$ | 2.51 ± 1.44 $^{cF}$ | 6.29 ± 0.82 $^{cE}$ | 8.84 ± 1.64 $^{cD}$ | 10.29 ± 2.69 $^{cD}$ | 8.78 ± 0.83 $^{cD}$ | 4.72 ± 0.92 $^{cEF}$ | 4.01 ± 2.18 $^{cEF}$ | 21.22 ± 2.02 $^{cC}$ |
| **2 mg/mL** | 70.98 ± 0.37 $^{aAB}$ | 69.47 ± 0.84 $^{bC}$ | 69.90 ± 0.32 $^{bBC}$ | 71.53 ± 0.46 $^{bA}$ | 49.91 ± 0.6 $^{bG}$ | 60.43 ± 0.68 $^{bDE}$ | 59.03 ± 0.82 $^{bE}$ | 53.42 ± 0.66 $^{bF}$ | 35.64 ± 0.98 $^{bH}$ | 14.13 ± 1.77 $^{bI}$ | 11.51 ± 1.14 $^{bJ}$ | 61.54 ± 0.61 $^{bD}$ |
| **3 mg/mL** | 72.43 ± 0.82 $^{aC}$ | 73.95 ± 0.23 $^{aB}$ | 74.03 ± 0.65 $^{aB}$ | 72.18 ± 0.28 $^{aCD}$ | 56.45 ± 0.82 $^{aG}$ | 71.29 ± 0.68 $^{aDE}$ | 73.66 ± 0.54 $^{aB}$ | 71.16 ± 0.64 $^{aE}$ | 73.14 ± 0.59 $^{aBC}$ | 64.15 ± 0.13 $^{aF}$ | 64.45 ± 0.66 $^{aF}$ | 79.45 ± 0.51 $^{aA}$ |
| ***Protein denaturation activity (%)*** | | | | | | | | | | | | |
| **0.5 mg/mL** | 29.30 ± 0.91 $^{cB}$ | 32.16 ± 0.33 $^{dA}$ | 21.30 ± 1.83 $^{dC}$ | 14.68 ± 0.98 $^{dE}$ | 10.65 ± 1.15 $^{dF}$ | 15.15 ± 0.36 $^{cE}$ | 6.03 ± 0.29 $^{cG}$ | 12.11 ± 0.17 $^{cF}$ | 14.01 ± 1.87 $^{dE}$ | 18.20 ± 0.44 $^{cD}$ | 14.27 ± 0.38 $^{cE}$ | 18.33 ± 0.39 $^{dD}$ |
| **1 mg/mL** | 41.16 ± 1.87 $^{bB}$ | 46.63 ± 0.40 $^{cA}$ | 33.44 ± 0.42 $^{cC}$ | 28.07 ± 0.40 $^{cD}$ | 15.38 ± 2.07 $^{cG}$ | 21.59 ± 3.39 $^{bEF}$ | 19.62 ± 0.38 $^{bF}$ | 15.09 ± 0.60 $^{bG}$ | 21.63 ± 1.22 $^{cEF}$ | 23.11 ± 0.99 $^{bE}$ | 26.48 ± 0.69 $^{bD}$ | 31.41 ± 0.15 $^{cC}$ |
| **2 mg/mL** | 53.61 ± 3.38 $^{aB}$ | 59.04 ± 0.39 $^{bA}$ | 42.51 ± 1.60 $^{bC}$ | 36.55 ± 3.14 $^{bD}$ | 28.38 ± 1.09 $^{bFG}$ | 32.39 ± 0.94 $^{aE}$ | 20.18 ± 1.92 $^{bI}$ | 15.72 ± 0.27 $^{bJ}$ | 30.88 ± 1.69 $^{bEF}$ | 23.99 ± 1.47 $^{bH}$ | 26.32 ± 1.78 $^{bGH}$ | 42.68 ± 1.10 $^{bC}$ |
| **3 mg/mL** | 58.13 ± 2.93 $^{aB}$ | 64.25 ± 1.00 $^{aA}$ | 48.94 ± 0.89 $^{aC}$ | 42.67 ± 0.85 $^{aE}$ | 32.75 ± 1.15 $^{aGH}$ | 35.62 ± 3.12 $^{aF}$ | 24.96 ± 0.94 $^{aI}$ | 19.62 ± 2.10 $^{aJ}$ | 34.37 ± 0.55 $^{aFG}$ | 31.68 ± 2.17 $^{aGH}$ | 31.4 ± 0.64 $^{aH}$ | 45.75 ± 1.27 $^{aD}$ |

ER, *Ecklonia radiata*; FV, *Fucus vesiculosus*; AN, *Ascophyllum nodosum*. Values are mean ± SD ($n = 3$). Different uppercase letters (A-D) indicate significant differences ($p < 0.05$) between different seaweed species at the same concentration, while lowercase letters (a-d) denote significant differences ($p < 0.05$) among different concentrations within the same seaweed species.

three distinct mechanisms, revealing complementary yet different aspects of their activity. In the DPPH radical scavenging assay, a marked concentration-dependent increase was observed across all species, consistent with the typical behavior of phenolic compounds (Molole et al., 2022). *E. radiata* consistently exhibited superior activity, which aligns with its well-documented high phenolic content. The hydrolysis pH significantly modulated this activity, with alkaline conditions proving optimal for radical scavenging capacity. At 3 mg/mL, *E. radiata*'s activity under pH 13 (168.21 ± 0.70 μg Trolox/mL) significantly ($p < 0.05$) exceeded that at pH 1 (143.54 ± 0.43 μg Trolox/mL), while showing similar values at pH 4 (142.31 ± 1.67 μg Trolox/mL) and pH 10 (144.01 ± 1.57 μg Trolox/mL). This pH-dependent pattern suggests that strong alkaline conditions most effectively release phenolics with superior radical scavenging capacity (Papadaki et al., 2022). In contrast, *F. vesiculosus* and *A. nodosum* showed less pronounced pH dependence, with maximum activities remaining substantially lower than *E. radiata*'s minimum values. The FRAP assay revealed a similar pH-dependent trend for electron-donating capacity. *E. radiata*'s performance was strongly enhanced under alkaline conditions, with the pH 13 hydrolysate at 3 mg/mL (349.84 ± 12.94 μg Trolox/mL) exceeding those at pH 1 (289.95 ± 12.94 μg Trolox/mL), pH 4 (291.02 ± 13.13 μg Trolox/mL), and pH 10 (284.73 ± 6.73 μg Trolox/mL). This 20–23% enhancement under strong alkaline conditions indicates more efficient phenolic liberation and may enhance their electron-transfer properties by deprotonation of hydroxyl groups to form phenolates. This ionization increases the nucleophilicity of these phenolics, making them more reactive and thus improving their extraction and potential antioxidant function, consistent with their inherently high hydroxyl group density and conjugated systems (Zhang et al., 2021). The minimal FRAP values of *F. vesiculosus* across all pH conditions (24.74 ± 0.65 to 101.56 ± 2.27 μg Trolox/mL) further highlight fundamental structural limitations in its phenolic constituents. In a striking divergence, the metal chelating activity revealed completely different structure-activity relationships and pH dependencies. *F. vesiculosus* and *A. nodosum* demonstrated superior chelating capacity that increased progressively with concentration, reaching 46–52 μg EDTA/mL at 3 mg/mL across all pH conditions. This pH-independent enhancement suggests their bound phenolic pools contain abundant metal-chelating motifs (e.g., carboxylates, ortho-dihydroxyl configurations) that are effectively liberated across the entire pH spectrum (Scarano et al., 2023). Conversely, the consistently low FICA activity (≤20.56 μg EDTA/mL) observed in *E. radiata* extracts, despite its high total phenolic content, is most parsimoniously explained by an intrinsic structural deficiency. The phenolic constituents of *E. radiata* appear to lack the spatial arrangements required for stable metal coordination, namely ortho-dihydroxyl (catechol) configurations or conjugated keto-hydroxyl motifs. Matrix masking by residual polysaccharides or proteins is an unlikely confound. The low-temperature precipitation step was applied consistently across all fractions and species, so any interference would affect all samples equally rather than selectively suppressing chelation in *E. radiata* alone. The persistence of low FICA activity across the full pH range further rules out a reversible, pH-dependent blockage, which indicates that if steric or ionic shielding were responsible, at least partial recovery of chelation potential would be expected at some pH. The absence of any such recovery indicates that the low metal-chelating capacity is a constitutive property of *E. radiata* phenolic repertoire, which appears to be optimized for radical scavenging rather than transition metal coordination.

For α-amylase inhibition, *E. radiata* demonstrated exceptional, dose-dependent activity with pronounced pH dependence. A pivotal finding of this study is that the pH condition during hydrolysis is a critical determinant for the α-amylase inhibitory activity of *E. radiata.* The hydrolysates prepared under alkaline conditions (pH 10 and 13) exhibited a significantly enhanced inhibitory potency (80.61 ± 2.40% and 82.71 ± 0.85%, respectively) compared to those from acidic hydrolysis (78.08 ± 0.39% at pH 1 and 67.07 ± 3.45% at pH 4) at a concentration of 3 mg/mL. This pronounced 'alkaline enhancement' effect reveals that the optimal strategy for preparing α-amylase inhibitors from *E. radiata* fundamentally differs from the neutral or mildly acidic conditions often reported for the activity of pre-extracted phenolic compounds. Our results highlight that the role of pH in an extraction process can be distinct from its role in a binding interaction. The dramatic boost in activity under alkaline conditions leads us to propose that the most effective α-amylase inhibitors in *E. radiata* are not freely accessible but are bound within the algal matrix via alkali-labile linkages. Phlorotannins, the primary polyphenols in brown algae, are frequently integrated into the cell wall, covalently linked to polysaccharides such as alginates through alkali-labile bonds (e.g., ester bonds) that are stable in acid but readily cleaved in base. Consequently, acidic hydrolysis (pH 1–4) liberates only a limited number of active compounds, whereas alkaline hydrolysis (pH 10–13) efficiently severs these linkages, resulting in a substantial increase in the concentration of free, active inhibitors. This substantial release of inhibitors under alkaline conditions produces a net effect of superior activity that may outweigh any potential negative impact of high pH on the binding affinity of individual compounds. Beyond the mere release of bound phenolics, the alkaline environment likely generates more potent inhibitory species. The harsh conditions, particularly at pH 13, promote oxidation and polymerization of the liberated phlorotannins, potentially yielding higher-molecular-weight derivatives. It is well established that larger phlorotannin polymers can engage in extensive multi-point interactions with the active-site cleft of α-amylase, leading to more potent and stable inhibition than smaller molecules. Accordingly, the superior performance of the alkaline hydrolysates is in part attributed to the in-situ formation of these optimized, high-affinity polymeric structures. The results for α-glucosidase inhibition revealed complex, non-monotonic patterns that varied markedly with pH. *E. radiata* showed the highest inhibition at pH 13 (19.42 ± 0.09%) and pH 4 (18.55 ± 0.20%) at 0.5 mg/mL, but these values decreased at higher concentrations. This unusual inverse concentration dependence, particularly evident under acidic conditions (11.25 ± 0.48% at pH 1, 3 mg/mL vs. 17.89 ± 0.09% at 2 mg/mL), may be attributed to two non-mutually exclusive mechanisms. First, colloidal aggregation at higher extract concentrations (Feng & Shoichet, 2006) can sequester enzyme molecules and produce apparently lower inhibition signals independent of true inhibitory potency. Second, hydrolysate-derived non-phenolic compounds (e.g., liberated oligosaccharides or phenolic-polysaccharide fragments) may weakly activate α-glucosidase at elevated concentrations, partially offsetting inhibitor activity (Copeland, 2000). The generally modest inhibition rates across all species and pH conditions indicate that potent α-glucosidase inhibitors are not a prominent feature of these bound phenolic fractions.

In the NO inhibitory assay, all species showed strong concentration-dependence, though with different pH optima. *E. radiata* achieved high inhibition (> 60%) at just 1 mg/mL across all pH levels, demonstrating consistently potent activity regardless of hydrolysis conditions. In contrast, *A. nodosum* required both a high concentration (3 mg/mL) and alkaline hydrolysis (pH 13) to achieve maximum efficacy (79.45 ± 0.51%), indicating that its most potent NO-scavenging compounds are tightly bound and require vigorous alkaline conditions for liberation. *F. vesiculosus* showed intermediate behavior, with moderate pH dependence and maximum activity (73.66 ± 0.54%) achieved under combined high concentration and alkaline conditions. The protein denaturation inhibition assay revealed that *E. radiata*'s acidic hydrolysates (pH 1: 58.13 ± 2.93%; pH 4: 64.25 ± 1.00% at 3 mg/mL) were significantly more effective than its alkaline fractions (pH 10: 48.94 ± 0.89%; pH 13: 42.67 ± 0.85%). This inverse relationship suggests that the phenolic compounds responsible for protein stabilization are structurally distinct. Their greater activity in acidic fractions suggests that they contain chemical bonds stable under acidic conditions but cleaved under alkaline conditions (e.g., certain glycosidic or ester bonds). The integrity of these alkali-labile bonds appears to be essential for preserving the specific three-dimensional structure (conformation) of the phenolics. This optimal conformation, in turn, enables highly effective

interactions with and stabilization of protein structures, thereby preventing denaturation. In contrast, the alkaline conditions likely break these bonds, altering the molecular conformation and diminishing their protein-stabilizing efficacy. *A. nodosum* showed a different pattern, with consistent moderate activity across pH conditions and highest efficacy at pH 13 (45.75 ± 1.27%), which suggests multiple anti-inflammatory mechanisms with different pH sensitivities.

In general, the non-monotonic and assay-specific pH response patterns observed across phenolic subclasses and biological endpoints suggest that hydrolysis pH modulates not only the extent but also the nature of phenolic release. The divergent pH optima observed across phenolic subclasses and bioassays argue against non-specific chemical artifacts, instead indicating selective liberation or transformation of functionally distinct phenolic pools. This selectivity provides a mechanistic basis for the contrasting bioactivity profiles observed under acidic and alkaline conditions, which suggests the functional heterogeneity of bound phenolics in brown seaweeds.

### 3.3. Matrix correlation and mantel linkage analyses of free and bound phenolic fractions

Pearson's correlation coefficients and Mantel's tests were used to evaluate relationships among individual bioactivity assays and to assess overall associations between phenolic composition and biological activities. As shown in Fig. 4(a), the inter-assay correlation matrix for the free phenolic fraction showed predominantly weak associations among the seven biological measurements, with most pairwise correlations exhibiting low-to-moderate coefficients. Only a limited number of assay pairs displayed high correlations ($r > 0.9$), among which the associations of α-amylase inhibition and NO inhibition with protein denaturation were the most pronounced ($p < 0.0001$). In addition, modest correlations ($0.8 < r < 0.9$) were observed for several relationships involving FRAP and α-glucosidase inhibition, whereas the remaining assay pairs showed weaker associations ($r \leq 0.7$).

Mantel analysis further indicated that only a subset of phenolic content indicators was significantly associated with individual bioactivities in the free phenolic fraction. Specifically, TPC exhibited a strong and significant positive association with DPPH scavenging activity, while similar positive linkages were observed for TFC and TPhC toward DPPH ($0.01 < p_m < 0.001$, $r_m > 0.25$). Moreover, TPC showed a notable positive association with α-amylase inhibition. In contrast, many other phenolic-bioactivity relationships were weak or non-significant ($p_m > 0.05$), and several negative associations were observed, indicated by dashed lines in the Mantel network, particularly between phenolic content measures and NO inhibition. Collectively, these results suggest that within the free phenolic fraction, only specific phenolic components are closely linked to selected antioxidant or enzyme-inhibitory activities, whereas most bioactivities appear to be largely independent of the overall phenolic content profile.

In comparison, the bound phenolic fraction (Fig. 4(b)) exhibited stronger and more coherent inter-assay correlations. The Pearson correlation matrix showed higher correlation coefficients and more significant relationships ($p < 0.0001$), indicating that bioactivities such as DPPH scavenging and FRAP, NO inhibition, protein denaturation, and α-amylase inhibition covaried more consistently in the bound extracts. In contrast, FICA and α-glucosidase inhibition displayed weak ($r < 0.5$) or negative correlations with other assays. Mantel analyses further revealed generally stronger linkages between phenolic content indicators and individual bioactivities in the bound fraction, as reflected by thicker and more prominent connections across most phenolic measures. Although negative associations were still detected, these were mainly associated with TFC, which may partly reflect its relatively low abundance in the bound phenolic extracts. Overall, the bound phenolic fractions exhibited a more structured, integrated correlation network than their free counterparts, indicating coordinated variation across multiple biological activities following hydrolysis. The strengthened correlation network in the bound fractions cannot be explained by phenolic abundance alone but rather reflects the release of a more functionally coherent phenolic assemblage upon hydrolysis. These results suggest that hydrolytic treatments selectively liberate phenolic pools with aligned functional properties, rather than uniformly increasing phenolic content across all bioactivities.

### 3.4. LC/Q-TOF MS/MS characterization of phenolic compounds in seaweed samples

Phenolic compounds in the seaweed samples were profiled using an untargeted LC-MS approach and tentatively annotated based on accurate mass measurements ($m/z$) and MS spectral information acquired in both positive and negative ionization modes. Compounds meeting stringent identification criteria (mass error < 5 ppm and PCDL library matching score > 80) were subjected to MS/MS fragmentation analysis for further structural confirmation (**SI. Table. S3).**

Untargeted LC-MS analysis revealed pronounced differences in phenolic composition among the three seaweed species, with a total of 133 compounds detected across all samples. A summary of their distribution across species and extraction conditions is presented in Table 2, while similarities and unique features among treatments are illustrated in the Venn diagrams (Fig. 5).

#### 3.4.1. Interspecific variability

Substantial interspecific variation was evident. *A. nodosum* exhibited the highest overall chemical richness (115 compounds), followed by *E. radiata* (104) and *F. vesiculosus* (99). Although several phenolic

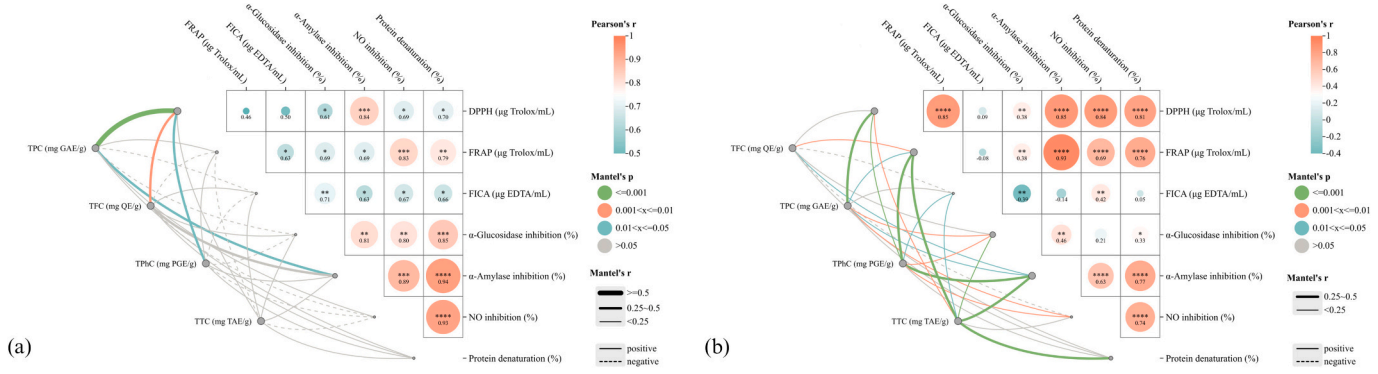


**Fig. 4. Interactive mantel test correlation heatmaps between content determination and biological activity tests.** (a) free fractions; (b) bound fractions. The heatmap shows the pairwise correlations between biological activity tests by Pearson correlation coefficient, with the stars showing the significant differences as $p < 0.05$ (*), $p < 0.01$ (**), $p < 0.001$ (***), $p < 0.0001$ (****). The lines denote mantel test results, with the line width represents Mantel's r statistic, the virtual and real lines represent negative and positive correlations, and the colors represent Mantel's *p*-values.

**Table 2**
**Distribution of tentatively identified phenolic compounds across species, fractions (free and bound), and pH-mediated extraction conditions.** Values represent the number of compounds detected under each condition.

| Phenolic class | *Ecklonia radiata* | | | | | *Fucus vesiculosus* | | | | | *Ascophyllum nodosum* | | | | |
|---|---|---|---|---|---|---|---|---|---|---|---|---|---|---|---|
| | Free fraction | Bound fraction | | | | Free fraction | Bound fraction | | | | Free fraction | Bound fraction | | | |
| | | pH = 1 | pH = 4 | pH = 10 | pH = 13 | | pH = 1 | pH = 4 | pH = 10 | pH = 13 | | pH = 1 | pH = 4 | pH = 10 | pH = 13 |
| **Flavonoids** | 21 | 17 | 16 | 24 | 17 | 13 | 16 | 18 | 16 | 22 | 20 | 24 | 20 | 22 | 21 |
| **Lignans** | 4 | 3 | 4 | 4 | 3 | 3 | 1 | 7 | 6 | 2 | 4 | 3 | 4 | 4 | 5 |
| **Other polyphenols** | 10 | 9 | 11 | 10 | 11 | 11 | 13 | 8 | 7 | 7 | 11 | 10 | 10 | 13 | 11 |
| **Phenolic acids** | 17 | 11 | 17 | 13 | 14 | 7 | 11 | 8 | 12 | 10 | 21 | 5 | 20 | 17 | 14 |
| **Stilbenes** | 1 | 1 | 2 | 0 | 2 | 3 | 1 | 2 | 2 | 1 | 0 | 3 | 2 | 2 | 2 |
| **Summary** | 53 | 41 | 50 | 51 | 47 | 37 | 42 | 43 | 43 | 42 | 56 | 45 | 56 | 58 | 53 |

Total unique compounds per species: *Ecklonia radiata* (104), *Fucus vesiculosus* (99), *Ascophyllum nodosum* (115).

compounds were commonly detected across species, a substantial proportion were species-specific, reflecting differences in phenolic biosynthesis and cell wall architecture. For example, compound **97** was characterized as gallic acid 4-O-glucoside, and compound **125** was 1-sinapoyl-2,2′-diferuloylgentiobiose. These compounds were exclusively detected in *F. vesiculosus* in both free and bound fractions. The former has previously been reported in several soft fruits (e.g., blackberries, blackcurrants, gooseberries, and blueberries) (Schuster & Herrmann, 1985), whereas the latter has been identified in broccoli (commercial cultivar Marathon) (Vallejo et al., 2003).

In addition, across most extraction treatments, flavonoids were the dominant phenolic class, aligning with the findings of Vinodkumar and Packirisamy (2023), who reported that the major class of polyphenolic compounds found in seaweed is flavonoids. In the free fractions, flavonoids accounted for 21, 13, and 20 compounds in *E. radiata*, *F. vesiculosus*, and *A. nodosum*, respectively, representing approximately 40%, 35%, and 36% of the total detected free phenolics in each species. Quercetin 3-O-xyloside (compound **31**) was detected in all species and is found in a number of food items, such as apples, and may serve as a potential biomarker for consumption of these food products (Kschonsek et al., 2018). However, it should be noted that this tentative annotation reflects chemical richness rather than quantitative abundance. Accordingly, the relatively high number of flavonoid-related annotations in the LC-MS dataset does not contradict the low TFC values obtained by colorimetric assay; as established in Section 3.1.1. Likewise, phenolic acids also contributed substantially to the compositional profile, particularly in *A. nodosum*, where 21 free phenolic acids were detected, exceeding the corresponding numbers in *E. radiata* (17) and *F. vesiculosus* (7). The relatively high abundance of phenolic acids in *A. nodosum* indicates a species-specific enrichment of low-molecular-weight phenolics, which may reflect differences in metabolic allocation or environmental adaptation strategies. In contrast, the comparatively lower representation of phenolic acids in *F. vesiculosus* suggests a distinct distribution pattern across subclasses despite similar overall compound richness. Such differential allocation may also influence functional properties, including antioxidant capacity and reactivity toward matrix components.

Comparisons across species under identical extraction conditions further demonstrated pronounced compositional divergence. Even when the total number of detected compounds was comparable among species, the proportion of shared features remained relatively low. For example, under acidic extraction (pH 1), although the total detected compounds were similar across *E. radiata* (41), *F. vesiculosus* (42), and *A. nodosum* (45), fewer than half of the compounds (19) were commonly shared (Fig. 5(a)), while a substantial fraction remained species-specific. This limited overlap indicates that comparable chemical richness does not equate to compositional similarity, but rather reflects distinct phenolic assemblages shaped by species-dependent biosynthetic pathways and matrix characteristics.

### 3.4.2. pH-dependent release behavior

Pronounced pH-dependent differences were evident within the bound fractions of each species. The Venn diagrams (Fig. 5f-h) clearly demonstrated limited overlap among pH treatments. For example, in *A. nodosum*, 45 compounds were detected at pH 1 and 58 at pH 10, yet only 27 compounds were shared between the two treatments. On the other hand, *F. vesiculosus* exhibited relatively consistent total compound numbers across pH treatments (42 at pH 1 and pH 13; 43 at pH 4 and pH 10). However, only 12 compounds were common to all bound extraction conditions, and 10 compounds when the free fraction was included. Thus, pH was found not only to influence the total number of detectable phenolic compounds but also to reshape their compositional identity.

The limited overlap among bound phenolic fractions extracted at different pH values suggests that phenolic compounds in brown seaweeds are associated with the matrix through heterogeneous binding mechanisms. Acidic conditions may preferentially disrupt acid-labile or weak non-covalent interactions, whereas alkaline extraction is more effective at cleaving ester-linked or other covalently bound phenolics, thereby releasing compounds that remain inaccessible under milder conditions. Similar pH-dependent release behavior has been reported for bound phenolics in terrestrial plant matrices and macroalgae, where phenolic compounds are known to associate with cell wall polysaccharides such as alginates, cellulose, and fucoidans (Acosta-Estrada et al., 2014; Deniaud-Bouët et al., 2014).

Although certain phenolic compounds were detected across multiple species and extraction conditions, the predominance of species-specific and pH-specific features highlights the strong influence of both intrinsic biological factors and extraction strategy on the observed phenolic profiles. Differences in cell wall architecture, phenolic biosynthetic pathways, and the extent of phenolic-polysaccharide interactions among seaweed species are likely key contributors to the observed interspecific variability.

## 3.5. Conclusion

This study provides a comprehensive evaluation of how pH-mediated hydrolysis governs the release, composition, and biological functions of bound phenolic compounds in brown seaweeds. By systematically examining extraction responses across acidic, neutral, and alkaline conditions, we demonstrate that bound phenolics constitute a functionally diverse, pH-sensitive reservoir that is largely inaccessible to conventional solvent extraction alone. The contrasting behaviors observed among *E. radiata*, *A. nodosum*, and *F. vesiculosus* underscore the critical role of species-specific cell wall architecture in dictating phenolic binding modes and release efficiency. Importantly, hydrolysis pH was shown to exert selective rather than uniform effects. Extraction pH governed not merely the quantity of released phenolics but the functional identity of the liberated fraction. Critically, Mantel-based network analysis confirmed that bound fractions released by

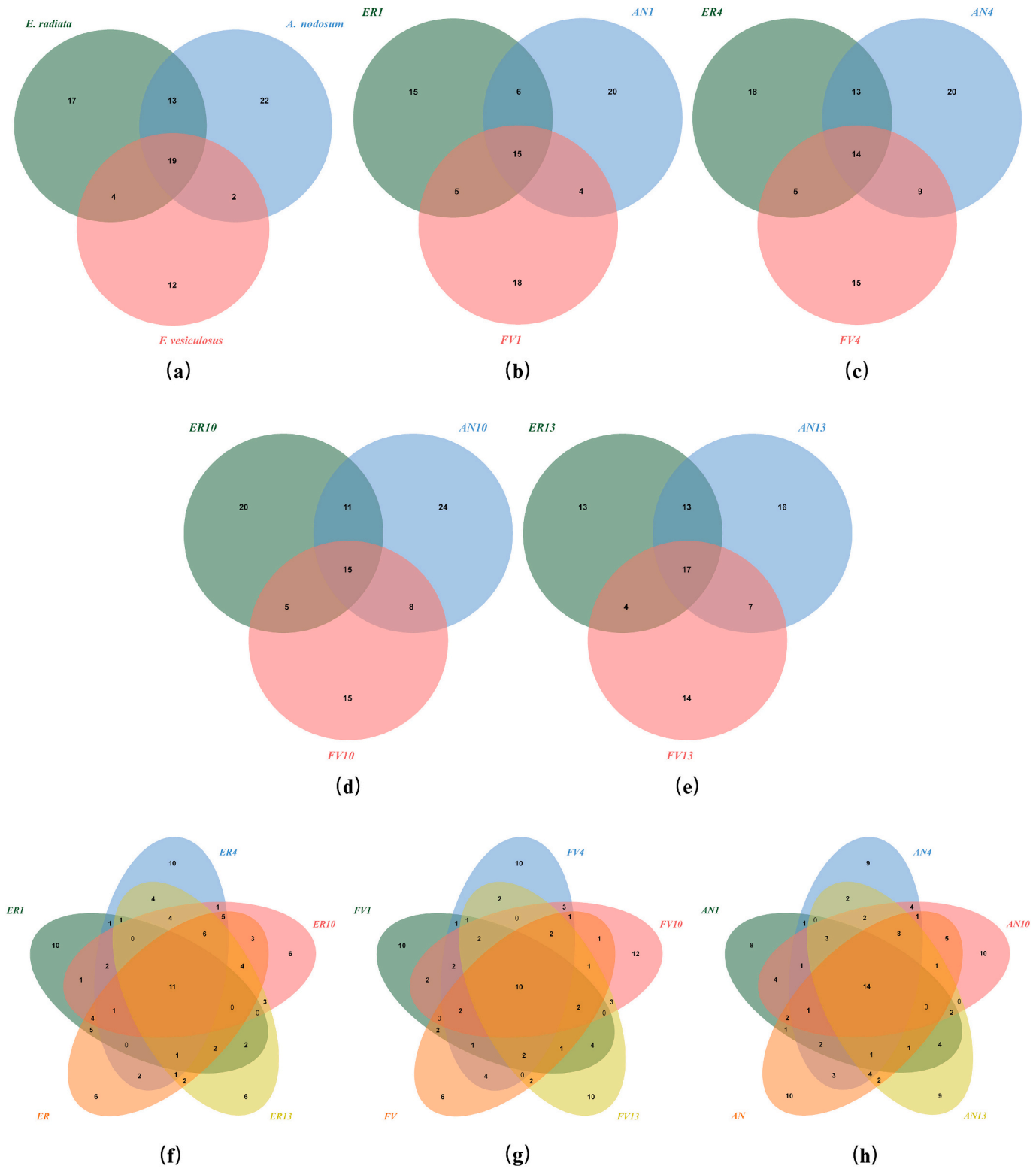


**Fig. 5. Venn diagram based on the detected and non-detected compounds in LC/Q-TOF MS/MS.** (a) Free phenolic fractions; (b) bound phenolic fractions under pH 1 treatment; (c) bound phenolic fractions under pH 4 treatment; (d) bound phenolic fractions under pH 10 treatment; (e) bound phenolic fractions under pH 13 treatment; (f) free and bound fractions of *Ecklonia radiata*; (g) free and bound fractions of *Fucus vesiculosus*; (h) free and bound fractions of *Ascophyllum nodosum*. ER, *Ecklonia radiata*; FV, *Fucus vesiculosus*; AN, *Ascophyllum nodosum*.

hydrolysis harbor functionally coordinated phenolic assemblages, rather thana non-selective mixture, providing mechanistic grounding for pH-targeted extraction design. In summary, extraction pH is not merely a technical parameter but a decisive selector of phenolic function. The pH-selectively principle established extends beyond the three species examined; other phenolic-rich marine biomass with complex polysaccharide cell walls is likely to harbor functionally distinct, pH-labile phenolic reservoirs whose valorization requires condition-specific

extraction strategies. This work therefore establishes a mechanistic framework for designing targeted extraction strategies tailored to specific bioactive applications. Future work should validate these extraction–bioactivity relationships in cell-based and in vivo models, and explore whether the functionally coherent phenolic assemblages identified here can be stably formulated for nutraceutical or pharmaceutical delivery systems, thereby advancing the systematic valorization of brown seaweeds as functional ingredients.

## CRediT authorship contribution statement

**Xinyu Duan:** Writing – original draft, Methodology, Investigation, Formal analysis, Data curation, Conceptualization. **Muthupandian Ashokkumar:** Writing – review & editing, Supervision, Conceptualization. **Frank R. Dunshea:** Writing – review & editing, Supervision, Conceptualization. **Hafiz A.R. Suleria:** Writing – review & editing, Validation, Supervision, Resources, Investigation, Funding acquisition, Conceptualization.

## Funding

The research was funded by the Australian Research Council through the "Discovery Early Career Award" (Grant No. ARC-DECRA-DE220100055) and by the University of Melbourne through the "Collaborative Research Development Grant" (Grant No. UoM-21/23).

## Declaration of competing interest

The authors declare that they have no known competing financial interests or personal relationships that could be perceived as a conflict of interest in connection with the work submitted.

## Acknowledgements

We would like to thank the Mass Spectrometry and Proteomics Facility from Bio21 Molecular Science and Biotechnology Institute at the University of Melbourne for their support throughout this study.

## Appendix A. Supplementary data

Supplementary data to this article can be found online at https://doi.org/10.1016/j.foodchem.2026.149408.

## Data availability

Data will be made available on request.

## References

Acosta-Estrada, B. A., Gutiérrez-Uribe, J. A., & Serna-Saldívar, S. O. (2014). Bound phenolics in foods, a review. *Food Chemistry, 152*, 46–55.

Akkarachiyasit, S., Charoenlertkul, P., Yibchok-Anun, S., & Adisakwattana, S. (2010). Inhibitory activities of cyanidin and its glycosides and synergistic effect with acarbose against intestinal α-glucosidase and pancreatic α-amylase. *International Journal of Molecular Sciences, 11*(9), 3387–3396.

Alloyarova, Y., Kolotova, D., & Derkach, S. (2024). Nutritional and therapeutic potential of functional components of brown seaweed: A review. *Foods and Raw Materials, 12*(2), 398–419.

Antony, A., & Farid, M. (2022). Effect of temperatures on polyphenols during extraction. *Applied Sciences, 12*(4), 2107.

Barzkar, N., Ivanova, S., Sukhikh, S., Malkov, D., Noskova, S., & Babich, O. (2024). Phenolic compounds of brown algae. *Food Bioscience, 62*, Article 105374.

Bone, K., & Mills, S. (2013). 2 - principles of herbal pharmacology. In K. Bone, & S. Mills (Eds.), *Principles and practice of Phytotherapy* (pp. 17–82). Churchill Livingstone.

Brand-Williams, W., Cuvelier, M. E., & Berset, C. (1995). Use of a free radical method to evaluate antioxidant activity. *LWT - Food Science and Technology, 28*(1), 25–30.

Brglez Mojzer, E., Knez Hrnčič, M., Škerget, M., Knez, Ž., & Bren, U. (2016). Polyphenols: Extraction methods, antioxidative action, bioavailability and anticarcinogenic effects. *Molecules, 21*(7), 901.

Catarino, M. D., Silva, A. M. S., & Cardoso, S. M. (2018). Phycochemical constituents and biological activities of fucus spp. *Marine Drugs, 16*(8), 249.

Cervin, G., Lindegarth, M., Viejo, R. M., & Åberg, P. (2004). Effects of small-scale disturbances of canopy and grazing on intertidal assemblages on the swedish west coast. *Journal of Experimental Marine Biology and Ecology, 302*(1), 35–49.

Chandimali, N., Bak, S. G., Park, E. H., Lim, H.-J., Won, Y.-S., Kim, E.-K., … Lee, S. J. (2025). Free radicals and their impact on health and antioxidant defenses: A review. *Cell Death Discovery, 11*(1), 19.

Cheng, A., Yan, H., Han, C., Chen, X., Wang, W., Xie, C., Qu, J., Gong, Z., & Shi, X. (2014). Acid and alkaline hydrolysis extraction of non-extractabke polyphenols in blueberries optimisation by response surface methodology. *Czech Journal of Food Sciences, 32*(3), 218–225.

Copeland, R. A. (2000). *Enzymes: A practical introduction to structure, mechanism, and data analysis*. Wiley.

Cotas, J., Leandro, A., Monteiro, P., Pacheco, D., Figueirinha, A., Gonçalves, A. M. M., … Pereira, L. (2020). Seaweed phenolics: From extraction to applications. *Marine Drugs, 18*(8), 384.

Deniaud-Bouët, E., Kervarec, N., Michel, G., Tonon, T., Kloareg, B., & Hervé, C. (2014). Chemical and enzymatic fractionation of cell walls from fucales: Insights into the structure of the extracellular matrix of brown algae. *Annals of Botany, 114*(6), 1203–1216.

Divekar, P. A., Narayana, S., Divekar, B. A., Kumar, R., Gadratagi, B. G., Ray, A., … Behera, T. K. (2022). Plant secondary metabolites as defense tools against herbivores for sustainable crop protection. *International Journal of Molecular Sciences, 23*(5), 2690.

Domínguez-Rodríguez, G., Marina, M. L., & Plaza, M. (2017). Strategies for the extraction and analysis of non-extractable polyphenols from plants. *Journal of Chromatography A, 1514*, 1–15.

Duan, X., Subbiah, V., Agar, O. T., Barrow, C. J., Ashokkumar, M., Dunshea, F. R., & Suleria, H. A. R. (2024). Optimizing extraction methods by a comprehensive experimental approach and characterizing polyphenol compositions of ecklonia radiata. *Food Chemistry, 455*, Article 139926.

Duan, X., Tuncay, A. O., & J, B. C., R, D. F., & Suleria, H. A. R.. (2025). Improving potential strategies for biological activities of phlorotannins derived from seaweeds. *Critical Reviews in Food Science and Nutrition, 65*(5), 833–855.

Farvin, K. S., & Jacobsen, C. (2013). Phenolic compounds and antioxidant activities of selected species of seaweeds from danish coast. *Food Chemistry, 138*(2–3), 1670–1681.

Feng, B. Y., & Shoichet, B. K. (2006). A detergent-based assay for the detection of promiscuous inhibitors. *Nature Protocols, 1*(2), 550–553.

Gonzales, G. B., Smagghe, G., Raes, K., & Camp, J. (2014). Combined alkaline hydrolysis and ultrasound-assisted extraction for the release of nonextractable phenolics from cauliflower (brassica oleracea var. botrytis) waste. *Journal of Agricultural and Food Chemistry, 62*(15), 3371–3376.

Gunathilake, K., Ranaweera, K., & Rupasinghe, H. P. V. (2018). In vitro anti-inflammatory properties of selected green leafy vegetables. *Biomedicines, 6*(4), 107.

Gunathilake, T., Akanbi, T. O., Suleria, H. A. R., Nalder, T. D., Francis, D. S., & Barrow, C. J. (2022). Seaweed phenolics as natural antioxidants, aquafeed additives, veterinary treatments and cross-linkers for microencapsulation. *Marine Drugs, 20*(7), 445.

Heffernan, N., Brunton, N. P., FitzGerald, R. J., & Smyth, T. J. (2015). Profiling of the molecular weight and structural isomer abundance of macroalgae-derived phlorotannins. *Marine Drugs, 13*(1), 509–528.

Heffernan, N., Smyth, T. J., FitzGerald, R. J., Soler-Vila, A., & Brunton, N. (2014). Antioxidant activity and phenolic content of pressurised liquid and solid–liquid extracts from four irish origin macroalgae. *International Journal of Food Science and Technology, 49*(7), 1765–1772.

Hendra, R., Army, M. K., Frimayanti, N., Teruna, H. Y., Abdulah, R., & Nugraha, A. S. (2024). A-glucosidase and α-amylase inhibitory activity of flavonols from stenochlaena palustris (burm.F.) bedd. *Saudi Pharmaceutical Journal, 32*(2), Article 101940.

Holdt, S. L., & Kraan, S. (2011). Bioactive compounds in seaweed: Functional food applications and legislation. *Journal of Applied Phycology, 23*(3), 543–597.

Irakli, M., Kleisiaris, F., Kadoglidou, K., & Katsantonis, D. (2018). Optimizing extraction conditions of free and bound phenolic compounds from rice by-products and their antioxidant effects. *Foods, 7*(6), 93.

Kedare, S. B., & Singh, R. P. (2011). Genesis and development of DPPH method of antioxidant assay. *Journal of Food Science and Technology, 48*(4), 412–422.

Khokhar, S., & Owusu Apenten, R. K. (2003). Iron binding characteristics of phenolic compounds: Some tentative structure–activity relations. *Food Chemistry, 81*(1), 133–140.

Koivikko, R., Loponen, J., Honkanen, T., & Jormalainen, V. (2005). Contents of soluble, cell-wall-bound and exuded phlorotannins in the brown alga fucus vesiculosus, with implications on their ecological functions. *Journal of Chemical Ecology, 31*(1), 195–212.

Krook, J. L., Riboldi, L., Birkeland, I. M., Stévant, P., Larsen, W. E., Rhein-Knudsen, N., … Horn, S. J. (2024). Acid preservation of the brown seaweed saccharina latissima for food applications. *Algal Research, 80*, Article 103524.

Krygier, K., Sosulski, F., & Hogge, L. (1982). Free, esterified, and insoluble-bound phenolic acids. 1. Extraction and purification procedure. *Journal of Agricultural and Food Chemistry, 30*(2), 330–334.

Kschonsek, J., Wolfram, T., Stöckl, A., & Böhm, V. (2018). Polyphenolic compounds analysis of old and new apple cultivars and contribution of polyphenolic profile to the in vitro antioxidant capacity. *Antioxidants (Basel), 7*(1), 20. https://doi.org/10.3390/antiox7010020

Kusmiyati, K., Hadiyanto, H., & Fudholi, A. (2023). Treatment updates of microalgae biomass for bioethanol production: A comparative study. *Journal of Cleaner Production, 383*, Article 135236.

Lee, Y. A., Cho, E. J., Tanaka, T., & Yokozawa, T. (2007). Inhibitory activities of proanthocyanidins from persimmon against oxidative stress and digestive enzymes related to diabetes. *Journal of Nutritional Science and Vitaminology, 53*(3), 287–292.

Lee, Z. J., Cundong, X., Ken, N., & Suleria, H. A. R. (2025). Unraveling the bioactive interplay: Seaweed polysaccharide, polyphenol and their gut modulation effect. *Critical Reviews in Food Science and Nutrition, 65*(2), 382–405.

Lee, Z. J., Xie, C., Duan, X., Ng, K., & Suleria, H. A. R. (2024). Optimization of ultrasonic extraction parameters for the recovery of phenolic compounds in brown seaweed: Comparison with conventional techniques. *Antioxidants, 13*(4), 409.

Lukova, P., Kokova, V., Baldzhieva, A., Murdjeva, M., Katsarov, P., Delattre, C., & Apostolova, E. (2024). Alginate from ericaria crinita possesses antioxidant activity and attenuates systemic inflammation via downregulation of pro-inflammatory cytokines. *Marine Drugs, 22*(11), 482.

Manohar, M., Lee, J. H., Park, H., Choi, Y. W., An, B. S., Albers, J., … Kim, M. (2025). Alkaline stable cross-linked anion exchange membrane based on steric hindrance effect and microphase-separated structure for water electrolyzer. *Materials Today Energy, 47*, Article 101739.

Molole, G. J., Gure, A., & Abdissa, N. (2022). Determination of total phenolic content and antioxidant activity of commiphora mollis (oliv.). *Engl. resin. BMC chemistry, 16*(1), 48.

Nicolescu, A., Bunea, C. I., & Mocan, A. (2025). Total flavonoid content revised: An overview of past, present, and future determinations in phytochemical analysis. *Analytical Biochemistry, 700*, Article 115794. https://doi.org/10.1016/j.ab.2025.115794

Obluchinskaya, E. D., Pozharitskaya, O. N., Zakharov, D. V., Flisyuk, E. V., Terninko, I. I., Generalova, Y. E., … Shikov, A. N. (2022). The biochemical composition and antioxidant properties of fucus vesiculosus from the arctic region. *Marine Drugs, 20*(3), 193.

Osawa, R., & Walsh, T. P. (1993). Effects of acidic and alkaline treatments on tannic acid and its binding property to protein. *Journal of Agricultural and Food Chemistry, 41*(5), 704–707.

O'Sullivan, A. M., O'Callaghan, Y. C., O'Grady, M. N., Queguineur, B., Hanniffy, D., Troy, D. J., … O'Brien, N. M. (2011). In vitro and cellular antioxidant activities of seaweed extracts prepared from five brown seaweeds harvested in spring from the west coast of Ireland. *Food Chemistry, 126*(3), 1064–1070.

Papadaki, E. S., Palaiogiannis, D., Lalas, S. I., Mitlianga, P., & Makris, D. P. (2022). Polyphenol release from wheat bran using ethanol-based organosolv treatment and acid/alkaline catalysis: Process modeling based on severity and response surface optimization. *Antioxidants, 11*(12), 2457.

Pasquet, P. L., Julien-David, D., Zhao, M., Villain-Gambier, M., & Trébouet, D. (2024). Stability and preservation of phenolic compounds and related antioxidant capacity from agro-food matrix: Effect of pH and atmosphere. *Food Bioscience, 57*, Article 103586.

Peng, Z., Wu, Y., Fu, Q., & Xiao, J. (2024). Free and bound phenolic profiles and antioxidant ability of eleven marine macroalgae from the South China Sea. *Frontiers in Nutrition, 11*, 1459757.

Poloczanska, E. S., Limpus, C. J., & Hays, G. C. (2009). Chapter 2 vulnerability of marine turtles to climate change. In , *Vol. 56. Advances in marine biology* (pp. 151–211). Academic Press.

Pufky-Heinrich, D., Roessiger, B., & Unkelbach, G. (2018). Base-catalyzed depolymerization of lignin: History, challenges and perspectives. In M. Poletto (Ed.), *Lignin - trends and applications*. IntechOpen.

Ratananikom, K., Juntaree, V., Wichaiyo, W., Khunluek, K., Premprayoon, K., & Kubola, J. (2024). In vitro evaluation of α-glucosidase and α-amylase inhibition in thai culinary vegetables. *Scientifica, 2024*, 3625267.

Rossi, L., Canala, B., Fifi, A. P., & Frazzini, S. (2024). In vitro evaluation of functional properties of extracts of fucus vesiculosus obtained with different conventional solvents. *Algal Research, 84*, Article 103787.

Scarano, A., Laddomada, B., Blando, F., De Santis, S., Verna, G., Chieppa, M., & Santino, A. (2023). The chelating ability of plant polyphenols can affect iron homeostasis and gut microbiota. *Antioxidants (Basel, Switzerland), 12*(3), 630.

Schuster, B., & Herrmann, K. (1985). Hydroxybenzoic and hydroxycinnamic acid derivatives in soft fruits. *Phytochemistry, 24*(11), 2761–2764.

Sobiesiak, M. (2017). Chemical structure of phenols and its consequence for sorption processes. In Marcos Soto-Hernandez, Mariana Palma-Tenango, & M. d. R. Garcia-Mateos (Eds.), Phenolic compounds-natural sources, importance and applications (pp. 3–26). IntechOpen.

Subbiah, V., Ebrahimi, F., Agar, O. T., Dunshea, F. R., Barrow, C. J., & Suleria, H. A. R. (2024). In vitro digestion and colonic fermentation of phenolic compounds and their antioxidant potential in australian beach-cast seaweeds. *Scientific Reports, 14*(1), 4335.

Subbiah, V., Ebrahimi, F., Duan, X., Agar, O. T., Barrow, C. J., & Suleria, H. A. R. (2024). Insights into the in vitro biological properties of australian beach-cast brown seaweed phenolics. *Food Science & Nutrition, 12*(11), 8956–8967.

Toth, G. B., & Pavia, H. (2001). Removal of dissolved brown algal phlorotannins using insoluble polyvinylpolypyrrolidone (PVPP). *Journal of Chemical Ecology, 27*(9), 1899–1910.

Trang Thuy, N. N., & Men, T. T. (2025). Phytochemical and bioactive analysis of extracted brown macroalgae (dictyota implexa) collected in Vietnam. *Biochemistry Research International, 2025*, 9461117.

Vallejo, F., Tomás-Barberán, F. A., & García-Viguera, C. (2003). Effect of climatic and Sulphur fertilisation conditions, on phenolic compounds and vitamin c, in the inflorescences of eight broccoli cultivars. *European Food Research and Technology, 216*(5), 395–401.

Vinodkumar, M., & Packirisamy, A. S. B. (2023). Effective isolation of brown seaweed flavonoids with their potential to inhibit free radicals and proliferative cells. *Journal of Inorganic and Organometallic Polymers and Materials, 33*, 3794–3804.

Wang, M., Leng, C., Zhu, Y., Wang, P., Gu, Z., & Yang, R. (2022). UV-B treatment enhances phenolic acids accumulation and antioxidant capacity of barley seedlings. *Lwt, 153*, Article 112445.

Xia, M., Li, M., Souza, T. S. P., Barrow, C., Dunshea, F. R., & Suleria, H. A. R. (2023). LC-ESI-QTOF-MS2 characterization of phenolic compounds in different lentil (lens culinaris m.) samples and their antioxidant capacity. *Frontiers in Bioscience-Landmark, 28*(3), 44.

Xie, C., Leeming, M. G., Lee, Z. J., Yao, S., Meene, A., & Suleria, H. A. R. (2024). Physiochemical changes, metabolite discrepancies of brown seaweed-derived sulphated polysaccharides in the upper gastrointestinal tract and their effects on bioactive expression. *International Journal of Biological Macromolecules, 272*(Pt 1), Article 132845.

Zhang, J., Hassane Hamadou, A., Chen, C., & Xu, B. (2021). Encapsulation of phenolic compounds within food-grade carriers and delivery systems by pH-driven method: A systematic review. *Critical Reviews in Food Science and Nutrition, 63*(19), 4153–4174.

Zhou, K., Yin, J., & Yu, L. (2006). ESR determination of the reactions between selected phenolic acids and free radicals or transition metals. *Food Chemistry, 95*(3), 446–457.